Computers and Chemical Engineering 149 (2021) 107285

Contents lists available at ScienceDirect

Computers and Chemical Engineering

journal homepage: www.elsevier.com/locate/compchemeng

Optimal design of controlled environment agricultural systems under market uncertainty

Shaylin A. Cetegen[a,b], Matthew D. Stuber[a,*]

[a] Process Systems and Operations Research Laboratory, Dept. of Chemical and Biomolecular Engineering, University of Connecticut, 191 Auditorium Road, Unit 3222, Storrs, CT 06269, USA
[b] Dept. of Chemical Engineering, Massachusetts Institute of Technology, 77 Massachusetts Ave., Cambridge, MA 02139, USA

ARTICLE INFO

Article history:
Received 23 December 2020
Revised 12 February 2021
Accepted 9 March 2021
Available online 13 March 2021

Keywords:
Semi-infinite programming
Robust optimization
Global optimization
Branch-and-bound
Sustainable agriculture

ABSTRACT

We present a novel methodology for the simultaneous robust design and scheduling of controlled environment agricultural (CEA) systems under multi-period risk. This problem is formulated as a semi-infinite program with several semi-infinite constraints pertaining to mean-variance risk exposure with uncertain covariance over each period in the planning horizon. The general model enables robust optimization of CEA systems for cultivation of any crop portfolio under any number of cultivation modes, with a solution that represents an optimal design and operating schedule that is robust to worst-case uncertainty. Therefore, this methodology provides a conservative basis for engineering and investment decision-making and represents, to our knowledge, the first robust optimization approach to CEA systems. Our approach effectively increases the robustness of CEA systems to market uncertainty, improves the long-term economics of CEA systems over naïve operating strategies, and validates the economic viability of single and multi-mode CEA production of distinct crop portfolios.

1. Introduction

Conventional agribusiness operations are inherently risky as their economic feasibility depends on highly uncertain factors such as weather and food supply and demand. Unpredictable environmental changes and extreme weather events such as droughts, floods, and fires pose direct threats to crop yields, which translate to significant revenue losses for agricultural producers over time (Deschênes and Greenstone, 2007; FAO, 2018). As the duration and frequency of such events are projected to rise into the foreseeable future, their impacts will continue to endanger the global food supply (Field et al., 2012). Further, as global population growth intensifies, increasing food demand is projected to outpace the capabilities of traditional outdoor agriculture systems (Fedoroff, 2015). As long as these trends persist, the compounding effects of greater weather variability and demand-driven market volatility will continue to endanger conventional agribusiness operations. The demand for increased food production under heightened uncertainty will not only increase pressure on existing agricultural operations, but also pose a broader challenge to food security. To ensure growing demand continues to be met under increasingly volatile conditions, alternative agricultural approaches are being considered to supplement traditional outdoor growing methods.

Controlled environment agriculture (CEA) is an alternative strategy in which crops are cultivated indoors in climate-controlled environments. Decoupling crop growth from environmental conditions through CEA presents an opportunity to alleviate the stress placed on exhaustible natural resources by existing food production practices while increasing local food production and improving food access and security (Benke and Tomkins, 2017). Increased consumer demand for year-round local availability of responsibly sourced fresh produce has already motivated the establishment of CEA operations across the United States, Europe, Asia, and Australia (Despommier, 2009; Butturini and Marcelis, 2020). The adoption of this alternative growing model has risen in recent years and is expected to grow significantly with rising consumer demand and climate awareness. It is estimated that the global vertical farming market alone, a subset of the global CEA market, is projected to reach $9.96 billion by 2025, expanding at a compound annual growth rate of more than 21% over the forecast period (Grand View Research, 2019). However, the high-risk low-reward nature of traditional agribusiness poses a challenge to the investment in and growth of this more environmentally and socially responsible alternative to traditional cultivation methods. To reap the benefits of CEA, the economic motivation for investment in this approach

* Corresponding author.
E-mail addresses: cetegen@mit.edu (S.A. Cetegen), stuber@alum.mit.edu (M.D. Stuber).

https://doi.org/10.1016/j.compchemeng.2021.107285
0098-1354/

Nomenclature

β	the set of odd years contained in project horizon
δ	the set of even years contained in project horizon
η	SIP auxiliary variable
γ	maximum objective function evaluation of all feasibility programs of the Grower's Model
μ	number of distinct growing modes
κ_z	set of indices for crops cultivated by mode z
Π	the discrete set of positive semidefinite matrices $\mathbf{M} \in M$
Ξ	interval matrix ($\in \mathbb{IR}^{n_c \times n_p}$) bounding $\mathbf{X}$ for the Grower's Model
a	cash flow discount rate
b	monthly capital financing interest rate
$C_{1,z}$	capital expenses of mode z that scale with capacity and are eligible for bulk discounting [USD/sq.ft.]
$C_{2,z}$	capital expenses of mode z that scale with capacity and are ineligible for bulk discounting [USD/sq.ft.]
$C_{3,z}$	capital expenses of mode z that do not scale with capacity [USD]
$C_{cap}(\mathbf{d})$	total capital expenses over project horizon as a function of $\mathbf{d}$ [USD]
$C_{op}(\mathbf{d}, \mathbf{X})$	total cash-discounted operating expenses over project horizon as a function of $\mathbf{d}$ and $\mathbf{X}$ [USD]
$C_{op,even,z}(\mathbf{X})$	operating expenses of even years of project horizon specific to cultivation mode z as a function of $\mathbf{X}$ [USD]
$C_{op,odd,z}(\mathbf{X})$	operating expenses of odd years of project horizon specific to cultivation mode z as a function of $\mathbf{X}$ [USD]
$C_{rev}(\mathbf{d}, \mathbf{X})$	total cash-discounted revenue over project horizon as a function of $\mathbf{d}$ and $\mathbf{X}$ [USD]
$C_{rev,even}(\mathbf{X})$	revenue of even years of project horizon as a function of $\mathbf{X}$ [USD]
$C_{rev,odd}(\mathbf{X})$	revenue of odd years of project horizon as a function of $\mathbf{X}$ [USD]
$\mathbf{d}$	optimization design decision variables ($\in \mathbb{R}^{n_d}$)
d_1	location of CEA system east(+)/west(−) of city center [miles]
d_2	location of CEA system north(+)/south(−) of city center [miles]
d_{z+2}	capacity of CEA system dedicated to cultivation mode z in [sq.ft.]
F_z	annual operating expenses specific to cultivation mode z that do not scale with capacity [USD]
g	objective function evaluation of Trader's Model feasibility problem
$G(\mathbf{d})$	location-based land cost model as a function of $\mathbf{d}$ [USD/sq.ft.]
H	interval set bounding η ($\in \mathbb{IR}$)
i	generic index used in NPV calculation and crop growing modes
$I_{op,j,z}$	operating expenses of quarter j for cultivation mode z that scale with capacity [USD/sq.ft]
$\mathbb{IR}$	set of all interval subsets of $\mathbb{R}$
j	quarter of planning horizon
k	iteration number of cutting plane algorithm
M	interval matrix bounding $\mathbf{M}$ ($\in \mathbb{IR}^{n_c \times n_c}$)
$\mathbf{M}$	covariance matrix of crop returns ($\in \mathbb{R}^{n_c \times n_c}$)
n_c	number of crops
n_d	number of design decision variables
n_l	capital financing repayment period [years]
n_p	number of quarters in a planning horizon
n_y	project horizon [years]
P	capital financing coefficient
$\mathbf{p}_{\min}$	minimum annual production of each crop as a fraction of demand
$\mathbf{p}_{\min}$	maximum annual production of each crop as a fraction of demand
$\mathbf{Q}$	diagonal matrix with entries representing the annual market demand of each crop ($\in \mathbb{R}^{n_c \times n_c}$) [pounds/year]
$\mathbf{r}$	expected quarterly returns on each crop ($\in \mathbb{R}^{n_c}$)
r_d	cash flow discount rate
$r_{\min}$	minimum portfolio return [%]
S	land cost at city center [USD]
$S_{\min}$	minimum land cost [USD]
t_r	tolerable risk [%]
u	risk [%]
V_i	capital discount factor of year i
$\mathbf{w}$	expected market price of each crop [USD]
x_{scale}	scaling factor for land cost depreciation in latitudinal direction from city center
$\mathbf{X}$	Grower's portfolio allocation ($\in \mathbb{R}^{n_c \times n_p}$)
$\mathbf{x}$	Trader's portfolio allocation ($\in \mathbb{R}^{n_c}$)
X	interval vector $[0, 1]^{n_c}$ bounding $\mathbf{x}$ for Trader's Model
y_{scale}	scaling factor for land cost depreciation in longitudinal direction from city center
$\mathbf{Y}$	diagonal matrix with entries representing annual yield of crop i [pounds/sq.ft.-year]
z	cultivation mode

must be strengthened through the development of tools offering improved system robustness to financial uncertainty.

In this work, we propose a novel design methodology with the potential to improve the economics and derisk the adoption of CEA technology. The paper will be structured as follows. In Section 2, background on established methodology is provided. In Section 3, our novel approach to optimizing CEA systems under market uncertainty is developed in detail. In Section 4, our approach is applied to two case studies and results are discussed. In Section 5, we conclude by summarizing the implications of our proposed approach. Additional details of the solution strategy and extended results can be found in the Supplementary Information.

2. Background

Established methods for decision-making under uncertainty, robust optimization, and portfolio optimization have been applied extensively across process systems engineering, finance, and operations research. In this section, we summarize the approaches we have integrated to develop a robust decision-making strategy for risk mitigation in CEA systems.

2.1. Decision-making under uncertainty in agriculture

Decision-making under uncertainty is the study of decision problems in which various possible states of uncertainty are known but insufficient information exists to assign probabilities of occurrence to each state. Several decision-making models designed to improve the efficiency of agricultural systems have already been developed and are summarized in three comprehensive reviews (Ahumada and Villalobos, 2009; Glen, 1987; Dury et al., 2012).

The review by Ahumada and Villalobos (2009) summarizes 20 deterministic and stochastic agricultural planning models based on optimization approaches used, types of crops modeled, and the scope of plans considered. Existing applications of design under uncertainty to traditional outdoor agriculture include use of a deterministic linear program (LP) with the objectives of satisfying market demand and maximizing profit to make planting decisions that provide a steady product supply over a long planning horizon (Hamer, 1994). Clustering heuristics and genetic algorithms have also been applied to determine the spatial allocation of plants in a greenhouse during multiple production periods to minimize cost and maximize space utilization (Annevelink, 1992) while fuzzy goal programming has been applied to solve land-use planning problems for the production of several seasonal crops during a planning year (Biswas and Pal, 2005). While most of these models have been developed for use in the design of highly specific agricultural applications, there also exist more generalized planning strategies such as that proposed by Nie et al. (2019) which uses data analytics and mixed-integer nonlinear modeling and optimization methods to find optimal solutions to the land-use problem. This strategy effectively promotes food production with reduced water and energy consumption and demonstrates robust performance under different climate scenarios. Overall, existing agricultural planning strategies overwhelmingly focus on the currently dominant method of traditional outdoor agriculture.

While the application of several existing agricultural planning models has yielded significant improvements in the performance of the systems for which they were designed, many of these models have been tailored to highly specific operations and cannot easily be adapted for general use in CEA investment decision-making (Ahumada and Villalobos, 2009; Benke and Tomkins, 2017). Further, the majority of existing agricultural planning models focus on traditional outdoor agriculture and do not explore mitigating the impacts of market uncertainty — the primary source of uncertainty impacting large-scale CEA systems. Because most existing models do not proactively account for the impact of future uncertainty on the system, they cannot guarantee that their solutions will remain feasible when future uncertainty is realized. Based on review of existing agricultural planning models, Benke and Tomkins (2017) identified the need for models providing accurate quantification of CEA economics and Ahumada and Villalobos (2009) called for models that include more realistic features for planning crop production for robustness to market uncertainty. For these reasons we have adopted a more flexible approach utilizing a single nonlinear economic objective to perform deterministic global optimization of the design and operation of CEA systems for cultivation of any crop portfolio under any number of cultivation modes for robustness to market uncertainty.

2.2. Robust optimization

Robust optimization is a proactive decision-making method that takes into account uncertainty from the design stage. First introduced by Ben-Tal and Nemirovski (1998) as a method to incorporate uncertainty into mathematical programming models, robust optimization has since been applied across process systems engineering and operations research communities to improve process scheduling under uncertainty (Li and Ierapetritou, 2008). In this work, to our knowledge, we present the first robust optimization approach to designing CEA systems.

To devise an effective robust agricultural planning strategy, sources of uncertainty with the greatest impact on the system of interest must be accounted for. In both traditional and CEA growing models, revenue is directly dictated by crop yields and the market prices at which crops are sold. As a result, crop yield and market price uncertainty should be considered from the design and planning stages to provide both growers and investors with robustness to future market uncertainty.

In traditional outdoor agriculture, crop yields vary drastically under weather uncertainty since non-ideal growing conditions often negatively impact crop health and growth rates, translating to reduced bottom line economic performance. Due to its significant impact, weather-driven agronomic yield uncertainty has been adopted as the primary uncertainty consideration in agricultural crop planning models to date (Ahumada and Villalobos, 2009). However, CEA involves growing crops indoors in climate-controlled environments where plants are exposed to optimal growing conditions and are shielded from weather impacts. This enables highly accurate yield prediction for well-established growing systems (Benke and Tomkins, 2017). As weather-driven agronomic yield uncertainty is eliminated through the controlled environment growing model, market uncertainty emerges as the primary source of uncertainty impacting the system and has therefore been adopted as the focus of this study.

2.3. Modern portfolio theory

To quantify uncertainty in our system as market risk, the modern portfolio theory (MPT) or mean-variance analysis definition of risk has been adopted. A recent study by Paut et al. (2019) demonstrated the efficacy of MPT as a method to quantify agronomic crop yield risk reduction by asset diversification for various crop classifications. However, this application of MPT only addressed agronomic risk reduction and did not consider the effects of diversification on mitigating economic uncertainty in agricultural systems. The elimination of crop yield uncertainty that is achieved through the CEA growing model enables the application of MPT to perform a purely economic analysis (Benke and Tomkins, 2017). This is the approach we have adopted in this study where we propose applying MPT in the development of investment decision-making and operations planning models to quantify the effects of diversification on mitigating economic uncertainty in commodities investment and CEA growing operations.

To achieve our stated objectives, we propose the joint application of MPT risk management and robust optimization as a novel approach to inform decision-making in commodities investment and CEA design and operations planning. To mitigate economic uncertainty and boost investment in the CEA sector, we have developed robust-optimal investment decision-making and operations planning frameworks from both a commodities trader's and a grower's perspective.

The trader's perspective is first presented as a direct implementation of established MPT and robust optimization methodologies. It is used to determine optimal investment allocations for portfolios of crop-specific commodities that minimize portfolio risk under worst-case uncertainty while delivering at least a minimum desired return on investment. While the Trader's Model is effective in identifying commodities investment portfolios (i.e., crop allocations) that are robust to worst-case risk, it is insufficient for optimizing the design and operation of highly complex CEA systems as a whole, which is desired to promote investment in and adoption of CEA technology. This problem, unlike the Trader's Model, is nontrivial because it requires solution of a bilevel program with a nonconvex outer program and multiple semidefinite inner programs. Since existing approaches could not be directly applied to solve this type of problem, a new methodology is developed herein for the global solution of a semi-infinite program (SIP) with multiple semi-infinite constraints. This Grower's Model was developed based on an extension of the Trader's Model and has been formulated generally to enable robust optimal decision-making for real-world CEA systems.

The proposed modeling frameworks and solution algorithms guarantee globally optimal solutions that enable stakeholders to reduce their risk exposure and financial vulnerability to worst-case market risk realizations, resulting in more stable economic performance of agricultural systems over the long term. The models' performance is assessed through two case studies involving cultivation of multi-crop portfolios. The broader implications of both approaches are discussed and the economic outcomes are compared against naïve investment and growing strategies from both perspectives. The risk reduction achieved through portfolio diversification and protection against worst-case risk achieved through robust optimization can be used to attract economic investment in this growing sector of the agriculture industry.

3. Method development

In this section, the robust optimization modeling frameworks are formalized from the trader's and grower's perspectives. First, the trader's perspective is considered as a straightforward application of robust portfolio optimization to CEA systems with crop-specific commodities as assets. The trader's approach is then extended to the grower's perspective where the simultaneous engineering design and operation of CEA systems is considered, enabling full-operation economic feasibility assessment of CEA systems.

3.1. Deterministic optimization from a trader's perspective

First, we develop a general method to generate agricultural commodities portfolios that are robust to a user-specified level of market uncertainty. This method can be applied to any agricultural portfolio for which historical crop pricing information is known and serves as a foundation for the development of our general approach to optimizing CEA systems under market uncertainty presented in Section 3.2.

To evaluate the economic feasibility of investment in agriculture from a commodities trader's perspective, robust optimization of investment portfolios comprised of crop-specific commodities has been performed. To do this, it was assumed that investors seek a risk-averse investment strategy—a foundational assumption of MPT—and that the risk (variance) associated with a given portfolio is calculated according to the MPT definition (Markowitz, 1952):

$$u = \mathbf{x}^{\mathrm{T}}\mathbf{M}\mathbf{x} \tag{1}$$

where $\mathbf{x} \in X \subset \mathbb{R}^{n_c}$ is the portfolio allocation of each crop $i = 1, \ldots, n_c$ with $X = [0,1]^{n_c}$ and $\mathbf{M} \in \mathbb{R}^{n_c \times n_c}$ is the covariance matrix of returns for all crop pairings over the investment period. Using this definition of risk, the trader seeks to minimize the maximum impact of uncertainty (risk) by finding a portfolio allocation that yields at least a minimum desired return while avoiding exposure to greater risk than their appetite.

The Trader's Problem is formulated as the following min-max problem:

$$\begin{aligned} f^* = \min_{\mathbf{x}\in X} \max_{\mathbf{M}\in M} \; & \mathbf{x}^{\mathrm{T}}\mathbf{M}\mathbf{x} - t_r \\ \text{s.t.} \; & \mathbf{r}^{\mathrm{T}}\mathbf{x} \geq r_{\min} \\ & \mathbf{1}^{\mathrm{T}}\mathbf{x} = 1. \\ & \mathbf{M} \succeq 0 \\ & M \in \mathbb{R}^{n_c \times n_c}, \; X = [0,1]^{n_c} \end{aligned} \tag{2}$$

where $t_r \in \mathbb{R}$ is the trader's tolerable risk level (user-specified parameter), $\mathbf{r} \in \mathbb{R}^{n_c}$ is the vector of expected returns on each crop, and $r_{\min}$ is the minimum required return on the portfolio.

To generate portfolios robust to a user-specified level of worst-case risk t_r, the model requires an input of historical pricing information for each commodity. Bounds on the uncertain covariance matrix of historical crop returns $\mathbf{M}$ were derived based on the assumption that future crop returns will not vary with respect to one another beyond the range by which they have done so historically over the same period during the past five years. The minimum and maximum values for each entry of the covariance matrix (i.e., each crop pairing) observed across all five historical covariance realizations considered under this assumption were selected as the lower and upper bounds of the real interval matrix $M \in \mathbb{IR}^{n_c \times n_c}$ (i.e., an $n_c \times n_c$-dimensional matrix whose elements are nonempty compact intervals).

Since the portfolio allocation variable vector $\mathbf{x}$ represents the fractions of the total portfolio that are to be invested in each crop, each component of $\mathbf{x}$ is bounded between 0 and 1 by components of X, and the vector sum is constrained to equal 1 (i.e., all available investment funds are allocated). Lastly, a constraint limiting the investment portfolio's minimum expected return $r_{\min}$ is included to ensure that risk mitigation efforts are only applied to the extent that at least a minimum economic return on investment can still be achieved. Note, since $r_{\min}$ is specified prior to any uncertainty analysis, this formulation may be infeasible (i.e., minimum required returns are too great). Further, since t_r is specified independently and prior to any uncertainty analysis, this problem (if feasible) provides the user with a "yes/no" determination of robustness. That is, a feasible solution is not robust if $f^* > 0$ as no portfolio could be found that minimizes the maximum impact of uncertainty and therefore results in greater risk exposure than tolerable.

Due to the complicated characterization of the feasible set of this optimization problem, the min-max program is not readily solvable using standard algorithms for nonlinear programs (NLPs), and therefore must be reformulated. Min-max programs are often reformulated as SIPs since several algorithms exist to estimate solutions of SIPs (Rustem and Howe, 2002). The min-max program is first reformulated as a bilevel program:

$$\begin{aligned} \eta^* = \min_{\eta \in H \subset \mathbb{R}, \mathbf{x}\in X} \; & \eta \\ \text{s.t.} \; & \mathbf{r}^{\mathrm{T}}\mathbf{x} \geq r_{\min} \\ & \mathbf{1}^{\mathrm{T}}\mathbf{x} = 1 \\ & \eta \geq \max_{\mathbf{M}\in M} \mathbf{x}^{\mathrm{T}}\mathbf{M}\mathbf{x} - t_r \\ & \quad \text{s.t.} \; \mathbf{M} \succeq 0 \end{aligned} \tag{3}$$

where η has been introduced as an auxiliary variable.

Significant efforts have been made to solve various classifications of bilevel programs using multiparametric programming (Pistikopoulos, 2009; Oberdieck et al., 2016). In multiparametric programming, the inner (multidimensional parametric) optimization problem is recast within a framework that seeks to characterize parametric optimal solution profiles as explicit mappings, with parameters corresponding to the decision variables of the outer optimization problem (Pistikopoulos, 2009). This allows the bilevel program to be recast into single-level deterministic optimization problems. Established methodologies for this approach are summarized in Oberdieck et al. (2016), and barring some examples of approximate solution maps for certain problems (e.g., see Dua et al., 2004; Grancharova and Johansen, 2006; Bemporad and Filippi, 2006), this approach has only been used broadly for problems with inner programs as LPs and quadratic programs (QPs) (Oberdieck et al., 2016). For bilevel problems involving a nonconvex outer program and a non-LP/QP inner program, such as the one we aim to treat in this application, established multiparametric programming methodology cannot be applied to furnish a globally optimal solution. As a result, this approach is not applicable to solve bilevel programs with an LP or NLP outer program and a semidefinite (SDP) inner program, as is the case for the

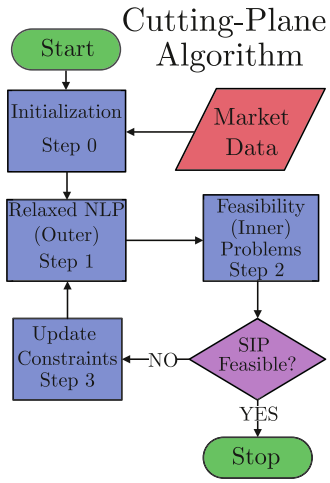

Fig. 1. The cutting-plane algorithm of Blankenship and Falk (1976) is illustrated in this flowchart as an iterative sequential solution of two NLPs. This algorithm is used to solve the semi-infinite programming problems for the trader's and grower's perspectives.

Trader's and Grower's Problems considered herein. The approach of Bemporad and Filippi (2006) for approximate solutions of multiparametric SDPs, may be applicable here, albeit not directly as it was developed only for linear functions. Further, since only a finite number of SDPs must be solved to optimality and can be done so very efficiently with available solvers, the advantages of developing a new multiparametric programming approach for this class of problems are not clear. For these reasons, we have decided to take an alternative approach and develop new solution strategies that exploit, as much as possible, efficient subprogram solvers to achieve our primary objective: the robust design of real-world CEA systems (i.e., the development and global optimization of the Grower's Model).

To achieve our objectives, we follow the approach of reformulating min-max and bilevel programs as SIPs (i.e., equivalent epigraph reformulations (Falk and Hoffman, 1977; Halemane and Grossmann, 1983; Žaković and Rustem, 2003; Stuber et al., 2014; Stuber and Barton, 2015)). The Trader's Problem bilevel program (3) is reformulated as the following SIP:

$$\begin{aligned} \eta^* = \min_{\eta\in H\subset\mathbb{R},\mathbf{x}\in X}\ & \eta \\ \text{s.t. } & \mathbf{r}^{\mathrm{T}}\mathbf{x} \geq r_{\min} \\ & \mathbf{1}^{\mathrm{T}}\mathbf{x} = 1 \\ & \mathbf{x}^{\mathrm{T}}\mathbf{M}\mathbf{x} - t_r - \eta \leq 0, \quad \forall\, \mathbf{M}\in M,\ \mathbf{M}\succeq 0. \end{aligned} \tag{4}$$

The first (inequality) and second (equality) constraints are affine functions of $\mathbf{x}$, and therefore are trivially convex on X. Since $\mathbf{M}$ is positive semidefinite, the semi-infinite constraint is convex with respect to $\mathbf{x}\in X$ and $\eta\in H\subset\mathbb{R}$ for every $\mathbf{M}$. Therefore, the SIP feasible set (and any discretization) is convex. The Trader's Problem SIP can trivially be solved using existing algorithms. However, the Grower's Model SIP is significantly more complicated, and a new solution approach has been proposed in Section 3.2.

We propose using the Blankenship and Falk (1976) cutting-plane algorithm (illustrated in Fig. 1) to solve (4) which involves an iterative procedure of sequentially solving two auxiliary programs. At iteration k, the first program solved is the *outer program* (Step 1 in Fig. 1):

$$\begin{aligned} (\eta^k,\mathbf{x}^k) \in \arg\min_{\eta\in H,\mathbf{x}\in X}\ & \eta \\ \text{s.t. } & \mathbf{r}^{\mathrm{T}}\mathbf{x} \geq r_{\min} \\ & \mathbf{1}^{\mathrm{T}}\mathbf{x} = 1 \\ & \mathbf{x}^{\mathrm{T}}\mathbf{M}\mathbf{x} - t_r - \eta \leq 0 \\ & \mathbf{M}\in\Pi^k, \end{aligned} \tag{5}$$

where $\Pi^k\subset M$ is a discrete set of positive semidefinite matrices $\mathbf{M}\in M$. Thus, (5) has a linear objective with affine and convex quadratic constraints. The second program solved is the *inner program* or *feasibility problem* (Step 2 in Fig. 1):

$$\begin{aligned} g^k = \max_{\mathbf{M}\in M}\ & (\mathbf{x}^k)^{\mathrm{T}}\mathbf{M}\mathbf{x}^k - t_r - \eta^k \\ \text{s.t. } & \mathbf{M}\succeq 0, \end{aligned} \tag{6}$$

which is an SDP. If $g^k > 0$, the corresponding optimal solution $\mathbf{M}^k$ is added to the discrete matrix set for the next iteration: $\Pi^{k+1} := \Pi^k\cup\{\mathbf{M}^k\}$ in Step 3 of Fig. 1. Otherwise, a feasible optimal solution $(\eta^k,\mathbf{x}^k)$ has been found and the algorithm terminates.

Theorem 3.1. *Let $H\in\mathbb{R}$, $X\in\mathbb{R}^{n_x}$ and $M\in\mathbb{R}^{n_x\times n_x}$ be nonempty. Define $\mathcal{F}_M=\{\mathbf{M}\in M:\mathbf{M}\succeq 0\}$. For any $\Pi^0\subset\mathcal{F}_M$, the algorithm of Blankenship and Falk (1976) converges to the optimal objective function value: $\{\eta^k\}\to\eta^*$.*

Proof. This result follows from compactness of $\mathcal{F}_M$ and continuity of $\mathbf{x}^{\mathrm{T}}\mathbf{M}\mathbf{x}-t_r-\eta$ on $X\times\mathcal{F}_M$, by Lemmas 2.2-2.3 of Mitsos (2011). □

Note, since the inner program is an SDP, its feasible set $\mathcal{F}_M$ is non-polyhedral and so convergence in finitely-many iterations cannot be guaranteed (Blankenship and Falk, 1976). The modification presented by Mitsos (2011) could be used, which involves solving an additional auxiliary problem to guarantee furnishing a feasible point in finitely-many iterations under relatively mild assumptions. For the cases considered herein, the Blankenship and Falk (1976) algorithm converged within a few iterations and therefore was adopted in favor of the Mitsos (2011) algorithm for its reduced computational complexity.

3.2. Deterministic optimization from a grower's perspective

The Trader's Model was extended to develop our novel Grower's Model that can be used to optimize the economic performance of CEA systems under controlled risk exposure. Like the Trader's Model, the Grower's Model is a general approach that enables optimization of CEA systems used to cultivate any crop portfolio for which historical crop pricing information is known. This method was developed for use as a decision-making and planning tool for the implementation of CEA systems under market uncertainty.

In contrast to the trader's perspective, the grower's perspective accounts for the capital and operating expenses involved in running a CEA system. The upfront capital investment in CEA systems can be significant but affords the grower a unique advantage over the trader, that is, the opportunity to profit from the value added by growing fresh produce from seed to plant. As the CEA industry continues to grow, decision-making models capable of mitigating uncertainty in CEA systems will be of increased demand as they provide critical insight to assessing the long-term financial sustainability of these operations. The Grower's Model presented herein represents, to our knowledge, the first robust optimization approach to CEA systems and is intended to provide design and operational insight for CEA technology adoption by enabling economic feasibility assessment of CEA systems under controlled risk exposure.

As applied in the trader's perspective, the strategy of achieving robustness to market volatility through asset diversification has similarly been applied to the grower's perspective where planting allocations are diversified over multiple grow periods, each under controlled risk exposure, while the economic performance of the entire system is simultaneously optimized over the CEA system's

project horizon. To optimize the Grower's Model subject to uncertainty, the following bilevel program with a nonconvex outer program and several SDPs as inner programs, must be solved to global optimality:

$$
\begin{aligned}
f^* = \max_{\mathbf{d}\in D, \mathbf{X}\in\Xi} \; & f_{\text{NPV}}(\mathbf{d},\mathbf{X}) \\
\text{s.t. } & \mathbf{1}^{\text{T}}\mathbf{x}_j = 1, \;\; j = 1,\ldots,n_p \\
& d_{z+2} = \left(\sum_{\zeta=1}^{\mu} d_{\zeta+2}\right)\left(\sum_{i\in\kappa_z} x_{ij}\right), \;\; j = 1,\ldots,n_p, z = 1,\ldots,\mu \\
& \mathbf{Q}\mathbf{p}_{\min} \le \left(\sum_{\zeta=1}^{\mu} d_{\zeta+2}\right)\left(\mathbf{Y}\sum_{j=1}^{4}\mathbf{x}_{j+4(q-1)}\right) \le \mathbf{Q}\mathbf{p}_{\max}, \\
& q = 1,\ldots,n_y \\
& 0 \ge \max_{j\in\{1,\ldots,n_p\}} \left\{ \max_{\mathbf{M}_j\in M_j} \mathbf{x}_j^{\text{T}}\mathbf{M}_j\mathbf{x}_j - t_r : \mathbf{M}_j \succeq 0, \right. \\
& \left. M_j \in \mathbb{IR}^{n_c\times n_c}, \;\; j = 1,\ldots,n_p \right\}.
\end{aligned} \tag{7}
$$

In this model, crop allocation decisions that are robust to a specified level of tolerable risk t_r are made on a quarterly basis while the design of the CEA system is simultaneously optimized to achieve a maximum net present value (NPV) over a user-specified project horizon of n_y years. This model includes design decision variables $\mathbf{d} \in \mathbb{R}^{n_d}$ with components representing the capacity dedicated to each cultivation mode (size of the proposed CEA system in square feet) and location (x and y coordinates in miles west/east and north/south of a user-specified urban center representing a location of peak demand) of the proposed CEA system. In the case of CEA systems with multiple cultivation modes, capacity is split between multiple decision variables $d_{z+2},\ z = 1,\ldots,\mu$, each representing the capacity dedicated to a single cultivation mode. Additionally, the model includes crop allocation decision variables $\mathbf{X} \in \mathbb{R}^{n_c\times n_p}$ for the first n_p quarterly grow cycles of operation which are repeated to span the entire duration of the project horizon over which the NPV is maximized and are bounded by the set $\Xi \in \mathbb{IR}^{n_c\times n_p}$ as the interval matrix with elements as the interval [0,1]. The growing allocation for the jth grow cycle is represented by the jth column vector of $\mathbf{X}$ denoted by $\mathbf{x}_j \in [0,1]^{n_c}$, κ_z is an index set corresponding to the crops cultivated by mode z, $\mathbf{Y} \in \mathbb{R}^{n_c\times n_c}$ is a diagonal matrix with entries representing the annual yield per square foot of each crop, $\mathbf{Q} \in \mathbb{R}^{n_c\times n_c}$ is a diagonal matrix with entries representing the annual market demand of each crop, and $\mathbf{p}_{\min}, \mathbf{p}_{\max} \in \mathbb{R}^{n_c}$ are respectively the minimum and maximum crop production limits for the CEA system.

The NPV of the system is calculated by the function:

$$
f_{\text{NPV}}(\mathbf{d},\mathbf{X}) = C_{rev}(\mathbf{d},\mathbf{X}) - (1+P)C_{cap}(\mathbf{d}) - C_{op}(\mathbf{d},\mathbf{X}), \tag{8}
$$

where C_{rev} is the lifetime revenue of the project, P is the capital financing coefficient, C_{cap} is the total capital cost of the project, and C_{op} is the lifetime operating cost of the project. Due to the structure of our formulation, which involves forecasting dynamic crop portfolios over a two-year planning horizon, annual revenues over each odd year of the project horizon are identical as are those over each even year of the project horizon. The same applies to operating expenses. Lifetime revenue and operating expenses are first calculated on an annual basis for odd and even years of the project horizon as shown here:

$$
C_{rev,odd}(\mathbf{X}) = \mathbf{w}^{\text{T}}\mathbf{Y}\sum_{j=1}^{4}\mathbf{x}_j \tag{9}
$$

$$
C_{rev,even}(\mathbf{X}) = \mathbf{w}^{\text{T}}\mathbf{Y}\sum_{j=5}^{8}\mathbf{x}_j \tag{10}
$$

$$
C_{op,odd,z}(\mathbf{X}) = \sum_{j=1}^{4} I_{op,j,z}(\mathbf{x}_j) \tag{11}
$$

$$
C_{op,even,z}(\mathbf{X}) = \sum_{j=5}^{8} I_{op,j,z}(\mathbf{x}_j), \tag{12}
$$

where $\mathbf{w} \in \mathbb{R}^{n_c}$ is the expected market price of each crop, $I_{op,j,z}(\mathbf{x_j})$ is the operating cost over quarter j for cultivation mode z that scales with system capacity (e.g., quarterly water bill for cultivation mode z). V_i is defined as a cash flow discount coefficient of year i accounting for a 12% cash flow discount rate to be applied to the revenue and operating expenses:

$$
V_i = (1+r_d)^{-i}, \tag{13}
$$

and $C_{rev}(\mathbf{d},\mathbf{X})$ and $C_{op}(\mathbf{d},\mathbf{X})$ are calculated from (9) to (12) as:

$$
C_{rev}(\mathbf{d},\mathbf{X}) = \left(\sum_{\zeta=1}^{\mu} d_{\zeta+2}\right)\left(C_{rev,odd}(\mathbf{X})\sum_{i\in\beta} V_i + C_{rev,even}(\mathbf{X})\sum_{i\in\delta} V_i\right) \tag{14}
$$

$$
\begin{aligned}
C_{op}(\mathbf{d},\mathbf{X}) = \left(\sum_{z=1}^{\mu} d_{z+2}\left(C_{op,odd,z}(\mathbf{X})\sum_{i\in\beta} V_i + \ldots \right.\right. \\
\left.\left. \ldots + C_{op,even,z}(\mathbf{X})\sum_{i\in\delta} V_i\right)\right) + F(\mathbf{d})\sum_{i=1}^{n_y} V_i,
\end{aligned} \tag{15}
$$

where we define $\beta = \{2x-1 : x \in \mathbb{N}, 1 \le 2x-1 \le n_y\}$ and $\delta = \{2x : x \in \mathbb{N}, 1 \le 2x \le n_y\}$, and $F(\mathbf{d})$ accounts for the annual operating expenses that are independent of capacity and cultivation mode. Capital expenses and capital financing are calculated by the equations:

$$
C_{cap}(\mathbf{d}) = \sum_{z=1}^{\mu} C_{1,z}(d_{z+2})^{0.9} + C_{2,z}d_{z+2} + G(\mathbf{d})d_{z+2} + C_{3,z} \tag{16}
$$

$$
G(\mathbf{d}) = S\exp\left(-x_{scale}(d_1)^2 + y_{scale}(d_2)^2\right) + S_{\min} \tag{17}
$$

$$
P = \frac{12b(1+b)^{12n_l}}{((1+b)^{12n_l}-1)}\sum_{i=1}^{n_l} V_i, \tag{18}
$$

where $C_{1,z}$, $C_{2,z}$, and $C_{3,z}$ are constants corresponding to each cultivation mode, z, that are independent of the design decision variables $\mathbf{d}$ and must be determined for each unique portfolio. For each cultivation mode z, $C_{1,z}$ is the sum of capital expenses that scale with capacity to which a 10% volume discount is applied (e.g., building materials with a bulk discount), $C_{2,z}$ is the sum of capital expenses that scale with capacity to which no discount is applied (e.g., building materials without a bulk discount), and $C_{3,z}$ is the sum of fixed capital expenses that do not scale with capacity (e.g., purchasing a fixed number of delivery trucks). A capital financing coefficient P, that is applied to capital expenses for NPV calculation, is defined in (18) and accounts for monthly amortization of capital expenses at a monthly interest rate b over the duration of the loan repayment period n_l in years. Capital financing has been amortized monthly while cash flows have been discounted annually.

The land cost model G is defined in (17) where S is the land cost per square foot at the city center (i.e., the presumed location of peak demand to which all products are assumed to be delivered), x_{scale} and y_{scale} are scaling factors representing the rate of land depreciation in the outward latitudinal and longitudinal directions from the city center, and $S_{\min}$ is the minimum land cost as the distance from the city center approaches infinity (i.e., no free or negative-cost land available). This Gaussian function returns the per-square-foot land acquisition cost; a non-discountable capital expense that scales with capacity. This term has been isolated from the $C_{2,z}$ constant in the capital expense model since, unlike $C_{2,z}$, it is dependent on the location decision variables (d_1, d_2). This dependency introduces nonconvexity to the capital expense and NPV models which necessitates the construction of custom affine relaxations (see Supplementary Information) to ensure that a globally optimal solution to the model can be obtained. Since this land cost model is symmetric about the longitudinal and latitudinal axes, multiple global optima arise. This land cost model (17) was created to represent a hypothetical cost model centered on a city with high land costs that decrease exponentially from the center; however, alternative models could be substituted in its place. The specific costs associated with the economic objective function of the Grower's Problem that are considered in the case studies presented herein are detailed in the Supplementary Information.

To summarize, capital expenses are dependent on all design decision variables $\mathbf{d}$ and independent of all crop allocation decision variables $\mathbf{X}$ since the total crop allocation to an individual cultivation mode remains constant over all n_p periods because constraints have been imposed to restrict modifying the system design after its initial construction (i.e., capacity dedicated to each cultivation mode and location of the CEA operation does not change after initial system construction). Operating expenses are dependent on all design decision variables $\mathbf{d}$ and crop allocation decision variables $\mathbf{X}$. Revenue is dependent on capacity decision variables $d_{z+2},\ z = 1, \ldots, \mu$, and crop allocation decision variables $\mathbf{X}$.

Following a similar development to the Trader's Problem, the Grower's Problem is then formulated as the following equivalent SIP:

$$
\begin{aligned}
f^* = \max_{\mathbf{d}\in D, \mathbf{X}\in\Xi}\ & f_{\mathrm{NPV}}(\mathbf{d}, \mathbf{X}) \\
\text{s.t. } & \mathbf{1}^{\mathrm{T}}\mathbf{x}_j = 1,\ j = 1, \ldots, n_p \qquad (19)\\
& d_{z+2} = \left(\sum_{\zeta=1}^{\mu} d_{\zeta+2}\right)\left(\sum_{i\in\kappa_z} x_{ij}\right),\ j = 1, \ldots, n_p, z = 1, \ldots, \mu \\
& \mathbf{Qp}_{\min} \le \left(\sum_{\zeta=1}^{\mu} d_{\zeta+2}\right)\left(\mathbf{Y}\sum_{j=1}^{4}\mathbf{x}_{j+4(q-1)}\right) \le \mathbf{Qp}_{\max},\ \ q = 1, \ldots, n_y \\
& \mathbf{x}_j^{\mathrm{T}}\mathbf{M}_j\mathbf{x}_j - t_r \le 0,\ \ \forall\, \mathbf{M}_j \in M_j \in \mathbb{IR}^{n_c\times n_c},\ j = 1, \ldots, n_p \\
& \mathbf{M}_j \succeq 0,\ j = 1, \ldots, n_p,
\end{aligned}
$$

in order to utilize the algorithmic framework of Blankenship and Falk (1976), illustrated in Fig. 1. The outer program of the Grower's Problem (19) determines the design and crop allocation decision variables to maximize NPV, the discounted sum of cash flows over the duration of the user-specified planning horizon, while the inner program selects covariance matrices for individual grow cycles that result in worst-case risk. Using this approach, the program determines the optimal design and crop allocations that maximize NPV when the worst-case market volatility of all grow cycles is realized. This approach ensures that risk exposure during any one grow period does not exceed a user-specified risk tolerance and delivers the maximum possible NPV for the system, ensuring peak economic performance under controlled risk exposure.

At iteration k of the cutting-plane algorithm, we solve the following *outer program* (Step 1 of Fig. 1) as an NLP relaxation of the original SIP (19), formulated as:

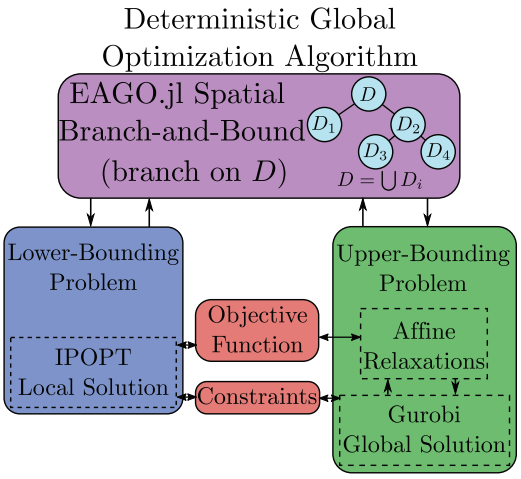

Fig. 2. The structure of the deterministic global optimization algorithm developed for solving the nonconvex outer program (20) of the Grower's Model is illustrated with its core routine as a customized spatial branch-and-bound algorithm that branches only on the design space D. This algorithm is guaranteed to solve (20) to global optimality in finite time.

$$
\begin{aligned}
(\mathbf{d}^k, \mathbf{X}^k) \in \arg\max_{\mathbf{d}\in D, \mathbf{X}\in\Xi}\ & f_{NPV}(\mathbf{d}, \mathbf{X}) \\
\text{s.t. } & \mathbf{1}^{\mathrm{T}}\mathbf{x}_j = 1,\ j = 1, \ldots, n_p \qquad (20)\\
& d_{z+2} = \left(\sum_{\zeta=1}^{\mu} d_{\zeta+2}\right)\left(\sum_{i\in\kappa_z} x_{ij}\right), \\
& j = 1, \ldots, n_p,\ z = 1, \ldots, \mu \\
& \mathbf{Qp}_{\min} \le \left(\sum_{\zeta=1}^{\mu} d_{\zeta+2}\right)\left(\mathbf{Y}\sum_{j=1}^{4}\mathbf{x}_j\right) \le \mathbf{Qp}_{\max} \\
& \mathbf{Qp}_{\min} \le \left(\sum_{\zeta=1}^{\mu} d_{\zeta+2}\right)\left(\mathbf{Y}\sum_{j=5}^{8}\mathbf{x}_j\right) \le \mathbf{Qp}_{\max} \\
& \mathbf{x}_j^{\mathrm{T}}\mathbf{M}_j\mathbf{x}_j - t_r \le 0,\ \forall \mathbf{M}_j \in \Pi_j^k,\ j = 1, \ldots, n_p.
\end{aligned}
$$

Since each of the matrices $\mathbf{M}_j \in \Pi_j^k$ are positive semidefinite, the quadratic inequality constraints are convex. Similarly, the first equality constraints are affine and therefore convex. Unfortunately, the second equality constraints related to the cultivation mode allocation are bilinear (nonconvex), the market share inequality constraints are bilinear (nonconvex), and f_{NPV} is likely nonconcave due to the existence of bilinear terms, summation of convex and concave terms, and the nonconvex Gaussian term (17). Therefore, (20) must be solved to guaranteed global optimality.

For this, we employ the extensible spatial branch-and-bound algorithm from EAGO v0.5.2 (Wilhelm and Stuber, 2018; 2020) with custom upper- and lower-bounding problems as illustrated in Fig. 2. The lower-bounding problem is defined simply as the NLP (20) with the given decision space corresponding to the current node in the branch-and-bound tree. We solve this problem to local optimality using IPOPT (Wächter and Biegler, 2006) through the Ipopt.jl package v0.6.3. The upper-bounding problem is defined using a *partial* relaxation procedure whereby we calculate affine relaxations of all nonlinear terms such that only affine and bilinear terms remain. In this case, since only C_{cap} involves such terms, only affine relaxations of the terms $C_{1,z}(d_{z+2})^{0.9},\ z = 1, \ldots, \mu$ and the function G, on their respective domains, are required. Details of how the affine relaxations are constructed can be found in the Supplementary Information. We then employ Gurobi v9.1.1

(Gurobi Optimization, 2020) with its nonconvex algorithm option to solve the resulting (potentially nonconcave) program.

The branch-and-bound algorithm is restricted to only branch on the **d** variables (i.e., those that are involved in the more complicated nonlinear expressions requiring custom relaxations) as Gurobi branches on both the **X** variables and **d** variables within the current node of the branch-and-bound tree. This novel selective branching strategy enables the combination of McCormick-based envelopes (McCormick, 1976) through custom routines in EAGO with the bilinear relaxations of Gurobi for an extremely effective spatial branch-and-bound algorithm capable of solving the large-scale Grower's Problems to guaranteed global optimality. All optimization problems are formulated in JuMP v0.21.4 (Dunning et al., 2017) in the Julia programming language v1.5.2 (Bezanson et al., 2017).

Since the Grower's Problem contains multiple semi-infinite constraints, at each iteration of the cutting-plane algorithm we solve in Step 2 of Fig. 1, the following n_p feasibility problems—corresponding to the lower-level programs of the original bilevel formulation— are solved to assess the feasibility of the design and multi-period crop allocations:

$$g_j^* = \max_{\mathbf{M}_j \in M_j} (\mathbf{x}_j^k)^{\mathrm{T}} \mathbf{M}_j \mathbf{x}_j^k - t_r \tag{21}$$
$$\text{s.t. } \mathbf{M}_j \succeq 0.$$

Since $\mathbf{x}_j^k$ is treated as constant (determined by (20)) and t_r is a user-defined parameter, the feasibility problems are SDPs, and therefore convex. Feasibility of a design $(\mathbf{d}^k, \mathbf{X}^k)$ is then satisfied for $\gamma \leq 0$, with

$$\gamma \equiv \max_{j \in \{1,\ldots,n_p\}} g_j^*.$$

For every $j \in \{1, \ldots, n_p\}$ such that $g_j^* > 0$, we add the corresponding $\mathbf{M}_j^*$ to the discrete set Π_j^k (i.e., $\Pi_j^{k+1} := \Pi_j^k \cup \{\mathbf{M}_j^*\}$) as Step 3 of Fig. 1. If an infeasible allocation for some grow period j is found, then the corresponding realization of uncertainty $\mathbf{M}_j$ is added to the discrete set Π_j of the corresponding SIP constraint in the upper program by the cutting-plane algorithm. The feasibility programs were solved using SCS (O'Donoghue et al., 2016; 2019). The convexity of the inner program ensures that the local optimum obtained using SCS is a guaranteed global optimum.

In summary, the Grower's Problem (19) is an SIP with $n_c \times n_p + \mu + 2$ upper-level decision variables corresponding to the system design and growing decisions, and n_p semi-infinite constraints each with $n_c \times n_c$ lower-level variables corresponding to uncertainty for each grow period. In Section 4, two Grower's Model case studies are considered with the largest exhibiting $n_c = 5$, $n_p = 8$, and $\mu = 2$, resulting in an SIP with 44 upper-level decision variables and 8 semi-infinite constraints each parameterized by 25-dimensional uncertainty sets. As such, this is a large-scale problem that is significantly more complex than any problem reported in the nonconvex SIP literature (Mitsos, 2011; Bhattacharjee et al., 2005b; 2005a). Although the semi-infinite constraints are convex, the SIP cannot be reduced to a standard NLP using a KKT reformulation approach, due to the semidefinite constraints.

As formulated, this model can easily be adapted to optimize the design and operation of CEA systems for cultivation of any number of crops n_c via any number of distinct cultivation modes μ; however, there exist some limitations to current formulation. For example, the current formulation of the Grower's Model assumes that all crops grown in the CEA system are cultivated over quarterly grow periods; however, the model can be adapted to account for grow periods of any duration by modifying the selection of historical pricing data used to construct bounds on **M** and updating the cash flow discounting and NPV formulations accordingly. As currently formulated, this model is not equipped to optimize the production of portfolios containing individual crops with distinct grow periods, although this could be implemented with careful consideration of risk and cash flows corresponding to each crop. Another limitation of the Grower's Model arises from the large discrepancy between the project horizon (i.e., 30 years) and planning decision (i.e., 3 months) timescales for which long-term planning of crop portfolios may be more suitably performed using a dynamic optimization approach. For this reason, crop planning decisions were only made for the first two years of the project horizon using our Grower's Model. These plans were then repeated 15 times to span the full 30-year project horizon. This approach was adopted in favor of making planning decisions for all 120 of the quarterly periods over the 30-year project horizon. This is because bounding the covariances of crop returns thirty years into the future based on long outdated historical pricing data may yield inaccurate results for this deterministic approach.

The presented Grower's Model represents a conservative method for CEA systems design since it delivers a design that is robust to the worst-case market uncertainty across all grow periods n_p. For this reason, the approach is intended primarily to aid in the initial design and planning of CEA systems. Once a CEA system design has been established, dynamic crop allocation and grow scheduling optimization would be recommended to maximize economic output under the chosen design accounting for the most up-to-date risk information.

4. Case studies

The Trader's Problem (4) and Grower's Problem (19) were each solved for two distinct case studies. To evaluate the proposed methodology across models and case studies, the robust design approaches employed were quantitatively compared to a naïve design approach, which was contrived to represent an assumed standard approach to decision-making in CEA systems design in the absence of CEA decision-making models.

4.1. Trader's perspective

4.1.1. Trader's perspective methods

The Trader's Problem (4) was applied in two case studies to analyze the effectiveness of our methodology against naïve investment strategies. The model was solved for two multi-crop portfolios using an input of historical pricing information in the form of monthly time-series data sourced from Tridge, a global trade ecosystem offering comprehensive market intelligence on agricultural products (Tridge, 2019). The two portfolios considered in this analysis were Portfolio A, containing lettuce, spinach, tomatoes, and strawberries; and Portfolio B, containing the same crops with the addition of mushrooms, which were included to introduce a second cultivation mode to the Grower's Model. Note that these specific crops were selected because they have been cultivated in existing CEA operations (Gómez et al., 2019; Miles and Chang, 2004) and open-access crop-specific market pricing data is readily available for them, enabling consistent analysis across both the trader's and grower's perspectives.

The Trader's Problem (4) was solved to determine robust optimal investment portfolios for quarterly periods over a two-year planning horizon. To study any potential impact of the starting month of the planning horizon on investment strategies (e.g., possible seasonal impacts), the described quarterly planning exercise was conducted with the starting month set to each calendar month (i.e., 12 independent studies). The expected risk and returns of the robust optimal solutions for each portfolio are reported and compared against the naïve strategy of investing in an equally distributed portfolio in Section 4.1.2.

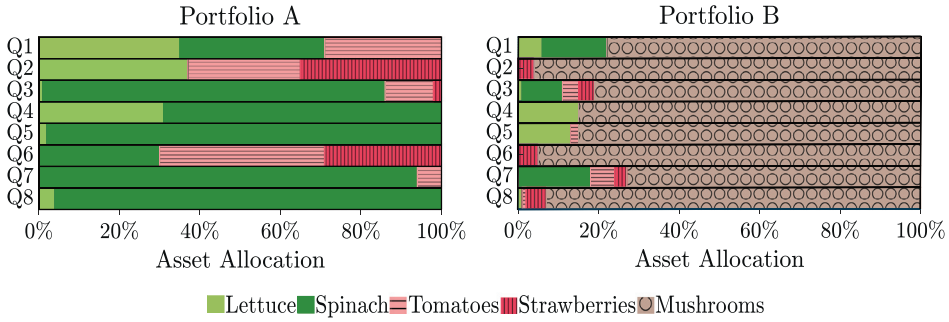

Fig. 3. Robust optimal dynamic portfolio allocations for the November 1, 2017–November 1, 2019 planning horizon for the Trader's perspective with 25% tolerable risk. Spinach is favored in Portfolio A and mushrooms are heavily favored in Portfolio B.

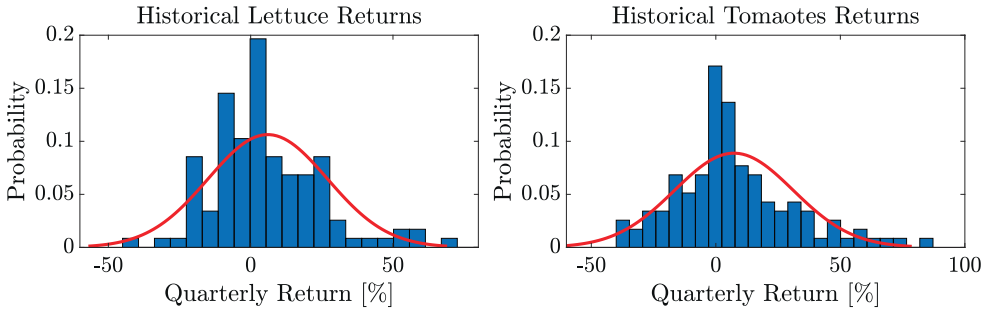

Fig. 4. Normal distributions were fit to historical crop returns and used to assess performance of robust and naïve portfolios from a returns perspective.

4.1.2. Trader's perspective results

Solving the trader's problem yielded robust feasible dynamic grow schedules for 31 out of the 33 unique quarterly periods simulated for Portfolio A and all 33 unique quarterly periods simulated for Portfolio B. Fig. 3 illustrates the results corresponding to the solution of the trader's problem for a single two-year planning horizon with a tolerable quarterly risk of $t_r = 25\%$ and minimum quarterly return of $r_{min} = 2\%$. These results show that optimization from the trader's perspective yields distinct investment portfolios over each quarter of the two-year investment period considered.

Once robust optimal dynamic portfolios were generated, their expected risk and returns were compared against those of the naïve strategy. For returns comparison, distributions of historically-observed quarterly returns on each crop were constructed from the past five years of data as shown for two crops in Fig. 4. These data were assumed to be representative of the future expected returns on each crop. Normal distributions were then fit to the historical data to obtain samplable approximations of the expected quarterly return on each crop. Finally, a Monte Carlo simulation with 10^5 realizations of market returns sampled from the normal distributions was performed to calculate the expected returns of the robust and naïve portfolios as shown in Fig. 6. Similarly, for risk comparison, normal distributions were constructed for the entries of $\mathbf{M}$ using the interval M by taking the means as the interval midpoints and the standard deviations as one-third of the interval radii. A Monte Carlo simulation with 5×10^5 realizations of market volatility $\mathbf{M}$ sampled as PSD matrices from these probability distributions was then performed to calculate the expected risk of the robust and naïve portfolios shown in Fig. 5.

Results of the Monte Carlo simulations show that robust optimal portfolios effectively reduced risk exposure with respect to naïve portfolios in all quarters for which robust solutions were obtained. Monte Carlo simulation results for risk and returns for Portfolio B over a single two-year planning horizon are shown in Figs. 5 and 6, respectively. These results only compare naïve and robust expected portfolio performance over a single two-year period simulated, but encompass the general trends observed throughout all quarters for which robust feasible solutions were obtained.

The results show that expected worst-case risk performance (highest risk) of the robust portfolios is lower than the best-case risk performance (lowest risk) of the naïve portfolios, demonstrating a clear advantage of the robust approach from a risk perspective. Robust portfolios also result in narrower risk distributions than naïve portfolios, meaning that the sensitivity of portfolio risk to market volatility is reduced using the robust optimization approach. The results also show that expected average returns for the robust portfolios are lower than those of the naïve portfolios, as was expected due to the risk-returns trade-off otherwise referred to as the price of robustness. It is notable, however, that the worst-case returns performance (lowest returns) of the robust portfolios is better than the worst-case returns performance (lowest return) of the naïve portfolios, demonstrating another advantage of this approach from a returns perspective. Through the robust optimization approach, the sensitivities of both portfolio risk and returns to market volatility are reduced; a potentially useful result for informing agricultural commodities investment decision-making.

The effectiveness of this approach over alternative approaches (i.e., the naïve strategy) from a risk perspective is illustrated through Fig. 7 which shows risk exposure of robust and naïve portfolios under worst-case and expected market conditions for all quarters simulated. Solutions of (4) provide portfolio allocations that are robust to worst-case market volatility. Robust and naïve expected risk was calculated using the robust and naïve portfolio allocations with a nominal covariance matrix that assumes each entry takes the element-wise median of the interval matrix of M. This nominal covariance assumption represents the market conditions under which all assets vary with respect to one another by the average amount they did over the past five years. This was included to contrast portfolio performance under nominal (expected) market volatility with that under worst-case market volatility. Finally, naïve worst-case risk was calculated by tuning the covariance matrix entries between the bounds on $\mathbf{M}$ to maximize naïve port-

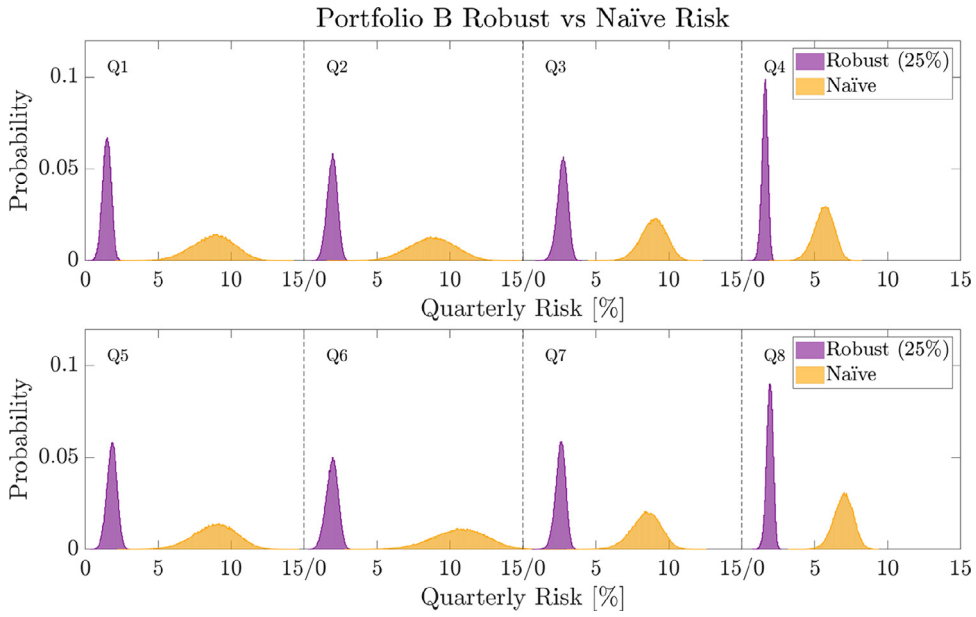

Fig. 5. Risk performance of Portfolio B is compared for naïve and robust (generated using 25% tolerable risk) portfolios for 5×10^5 realizations of expected market behavior over the March 1, 2018–March 1, 2020 planning horizon. Robust portfolios show narrower distributions and significantly reduced mean risk.

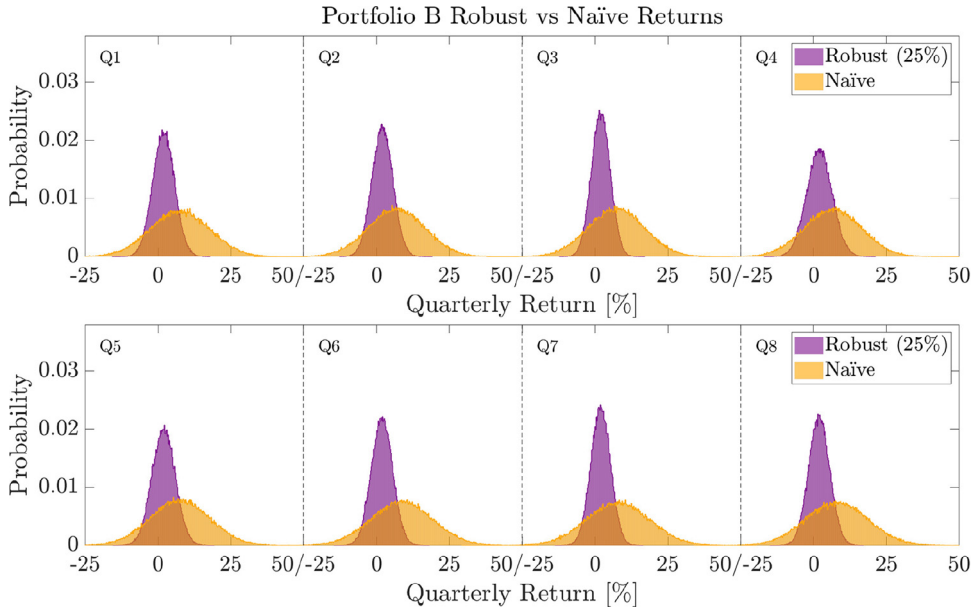

Fig. 6. Returns performance of Portfolio B is compared for naïve and robust (generated using 25% tolerable risk) portfolios for 5×10^5 realizations of expected market behavior over the March 1, 2018–March 1, 2020 planning horizon. Robust portfolios show narrower distributions but lower mean expected returns.

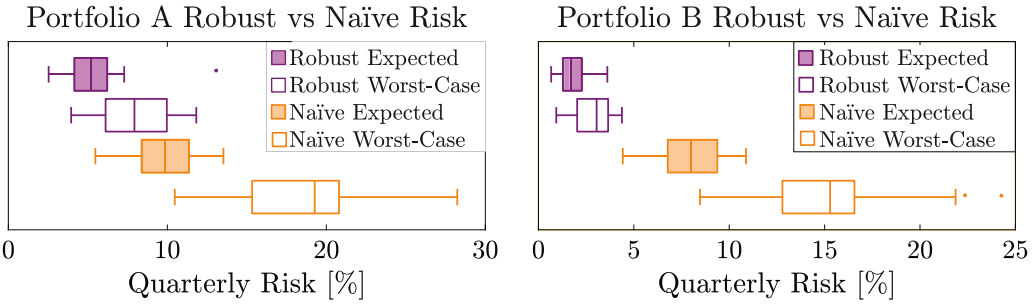

Fig. 7. Risk is compared between robust and naïve portfolios under expected and worst-case market conditions for Portfolios A and B.

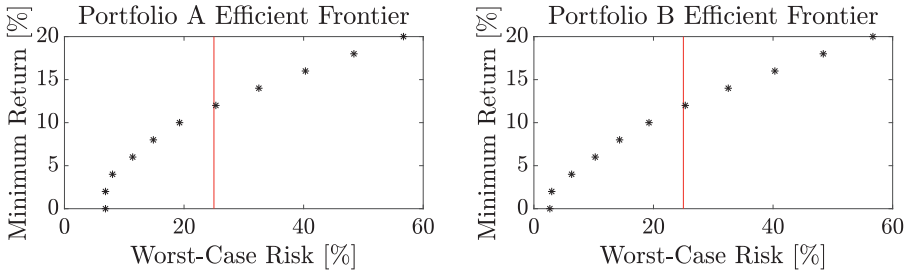

Fig. 8. Minimum returns vs. worst-case risk trade-off for Portfolios A and B are shown with solutions below 25% tolerable risk (vertical red lines) representing robust optimal solutions and solutions above 25% tolerable risk representing non-robust optimal solutions. (For interpretation of the references to color in this figure legend, the reader is referred to the web version of this article.)

folio risk. This represents the upper-bound of naïve portfolio risk that can be observed for these crop portfolios.

As expected, and as shown in Fig. 7, it was observed that for a given investment strategy (i.e., naïve or robust), portfolio risk exposure was lower under expected market conditions than under worst-case market conditions. By applying the robust optimization strategy, risk was reduced by an average of 37% for Portfolio A and 77% for Portfolio B compared against the naïve strategy under expected market volatility. Under worst-case market volatility, the robust portfolios offer an average risk reduction of 51% for Portfolio A and 81% for Portfolio B over naïve portfolios. It is also interesting to note that the risk exposure of the robust portfolios under worst-case market conditions was lower than that of the naïve portfolios under expected market conditions for 68% of Portfolio A quarters and 100% of Portfolio B quarters.

The goal of implementing robust portfolio optimization is to mitigate uncertainty, accounted for as variance/risk in this case. Such uncertainty mitigation, however, comes at the cost of reduced returns. Therefore, it was expected that robust portfolios would reduce investors' exposure to risk while also reducing their expected returns. The results observed from the trader's approach agree with this expectation since returns were reduced by an average of 66% for Portfolio A and 74% for Portfolio B compared against the naïve strategy under expected market volatility.

The minimum portfolio return used to solve (4) was arbitrarily set to 2% for this study. The risk-returns trade-offs of the Trader's Model for Portfolios A and B shown in Fig. 8, however, indicate that it is possible to set the minimum return up to 12% for each portfolio while keeping worst-case risk exposure under 25% (i.e., still obtaining a robust optimal solution of (4)). This analysis demonstrates that while our approach is effective at drastically reducing risk exposure at the expense of reduced returns, the same is possible to a lesser extent (i.e., lower risk reduction with lower returns reduction), which is why performing this analysis can be useful in identifying a risk-returns trade-off that is most desirable to investors based on their individual risk appetites and financial considerations.

Comparison of robust and naïve portfolio performance between Portfolios A and B show that the robust investment approach is an effective risk mitigation strategy. The extent to which portfolio risk exposure can be reduced, however, depends on the assets that comprise the portfolio. Since the robust approach offers risk reduction at the cost of portfolio returns, that trade-off should be assessed on a case-by-case basis for unique portfolios before choosing one investment strategy over another.

4.2. Grower's perspective

4.2.1. Grower's perspective methods

Deterministic global optimization of a large-scale CEA system was performed to investigate the economic viability of this emerging alternative approach to traditional outdoor agriculture from a grower's perspective. The Grower's Problem (19) was applied in two case studies to analyze the effectiveness of our methodology against alternative strategies. The model was solved to generate robust optimal designs and crop portfolios for CEA systems used to cultivate Portfolio A and Portfolio B crops under controlled risk exposure.

The capital and operating expense models used in this study were adapted from existing economic feasibility studies of CEA systems. In a detailed economic feasibility analysis of controlled environment lettuce and tomato cultivation, it was found that 98% of the total capital expenses were attributed to structure, illumination, horticulture, and air and thermal management costs while 98% of the total operating expenses were attributed to labor, energy, and horticulture costs (Zeidler et al., 2017). Specific expense models used for the Grower's Model case studies were based on a detailed cost breakdown for construction and operation of a large-scale CEA system presented by Zeidler et al. (2017). Costs from this study were normalized to a per-square-foot-of-land-footprint basis for use in our model. Since the Zeidler et al. (2017) study involved cultivation of lettuce and tomatoes only, but our study involved additional crops, it was assumed that spinach growing costs were equal to lettuce growing costs and strawberry growing costs were equal to tomato growing costs.

Structural capital expenses considered in this model include land acquisition and construction costs. Construction costs were derived from the Zeidler et al. (2017) study. Land acquisition costs were derived using a custom approach in which a location-based cost model (17) was generated using local land-cost data and incorporated into the nonlinear objective function through the capital expense model. Specifically, a multivariate Gaussian distribution was fit to normalized land-cost data over a geographic site selection region of interest. The Grower's Model case studies presented herein assume site selection within the greater Boston area. Land acquisition costs are the only capital expenses considered in the capital expense model that scale with capacity but do not qualify for volume discounting. All other capital expenses considered herein are either volume-discountable expenses that scale with capacity, non-volume-discountable expenses that scale with capacity but are independent of location decision variables, or fixed capital expenses that do not scale with capacity, which respectively correspond to constants $C_{1,z}$, $C_{2,z}$, and $C_{3,z}$ of the the capital expense model (16).

The Grower's Problem (19) with portfolio-specific capital and operating expense models was solved for each portfolio under variable tolerable quarterly risk levels. To assess the performance of this approach, the economic performance (i.e., NPV) corresponding to a solution to the Grower's Model, which represents a robust optimal design with robust optimal crop allocations (RO/RO), was compared against that of three alternative strategies: RO/N, RO/O, and O/O. The RO/N strategy represents a system that implements

Table 1
The solution times (s) for the Grower's Problem (19) for each portfolio are tabulated over the range of tolerable risk levels considered. In the worst case, these problems can be solved within a few minutes using the proposed algorithm. Portfolio A consists of 35 upper-level (design) decision variables and 8 semi-infinite constraints each parameterized by 16-dimensional uncertainty sets. Portfolio B consists of 44 upper-level (design) decision variables and 8 semi-infinite constraints each parameterized by 25-dimensional uncertainty sets.

Tolerable risk	10%	14%	21.75%	22.5%	23%	25%
Portfolio A	–	–	133.05	15.953	9.254	4.395
Portfolio B	288.66	379.20	8.879	5.406	5.191	6.236

a robust optimal design with naïve crop allocations substituted in place of the robust allocations. The comparison between RO/RO and RO/N performance was included to quantify the value of intelligently choosing crop allocations. The RO/O strategy represents a system that implements a robust optimal design with crop allocations that have been optimized to maximize NPV without risk consideration. The comparison between RO/RO, and RO/O was included to assess the price of robustness associated with considering market uncertainty only at the design stage (i.e., the price of implementing a robust design and subsequently making crop allocations without consideration for uncertainty). Finally, the O/O strategy represents a system that implements optimal design and crop allocations obtained without risk consideration. The comparison between RO/RO and O/O was included to assess the full price of robustness for this problem (i.e., the price of implementing a robust design and robust allocations versus a design that did not consider uncertainty at all). To further demonstrate the robustness of the Grower's Model, the risk performance of robust and naïve allocations under expected market behavior was also compared. All problems were solved on a personal workstation running Windows 10 v20H2 operating system with an Intel Core i7-5960x (8 core/16 thread) CPU operating at 4.3 GHz with 32 GB of RAM. Solution times were measured as an average of five runs for each case to quantify the computational performance of the proposed method.

4.2.2. Grower's perspective results

Solution of the Grower's Problem yielded robust optimal designs and dynamic grow schedules (robust optimal allocations) for CEA systems used to cultivate both crop portfolios. The NPVs of the robust optimal designs were positive over the 30-year project horizon considered, which indicates an economically feasible system was identified for both cases. The CPU times for each experiment are reported in Table 1. To assess the performance of this method, a comparison of the Portfolio A and Portfolio B results is shown in Table 2, where the NPV of the Grower's Problem solution (i.e., RO/RO case) is compared against the three other scenarios: RO/N, RO/O, and O/O.

The NPVs corresponding to solutions of the Grower's Problem (19), which represent robust optimal designs with robust optimal allocations (RO/RO), are reported in Table 2 for a range of tolerable risk levels. NPVs were then calculated for the robust optimal designs with naïve crop allocations substituted in place of the robust allocations (RO/N). The RO/N results yielded, on average, a 168% decrease in NPV for Portfolio A and a 163% decrease in NPV for Portfolio B. This means that the RO/N cases yield a negative NPV, which indicates an economically infeasible design. This result demonstrates that for a fixed design, sensitivity of the NPV to crop allocations can be significant, and in some cases, as observed here, can make the difference between an economically feasible and economically infeasible system.

A second comparison was made by fixing the design variables at an obtained robust optimal design and optimizing crop allocations to maximize NPV without considering risk (RO/O). As this problem was less constrained than the RO/RO case, it was expected that the resulting NPV of this case would be greater, assuming the risk constraints were active at the robust optimal solutions. The difference between the NPVs of the RO/RO and RO/O cases is the marginal cost of considering risk, (i.e., the price of robustness of crop allocations). The RO/O results yielded, on average, a 4.8% increase in NPV for Portfolio A and a 0.3% increase in NPV for Portfolio B. The lower improvement for Portfolio B is due to the relatively lower sensitivity of the design to risk and the greater degree of coupling between the design and crop allocations due to having mixed growing modes.

Lastly, the optimal design with optimal allocations (O/O) case was considered. In this case both the design and crop allocations are optimized without risk constraints. Since the crop allocations $\mathbf{X}$ are considered in risk calculations and the design $\mathbf{d}$ is not, it was expected that for greater tolerable risk levels, economically equivalent designs could be obtained for the considered cases, and therefore the O/O results could be identical to the RO/O results (and even the RO/RO results if the risk constraints were inactive). The O/O results yielded, on average, a 7.1% increase in NPV for Portfolio A and a 42.9% increase in NPV for Portfolio B over the RO/RO results. Further, the O/O results yielded, on average, a 2.2% increase in NPV for Portfolio A and a 42.6% increase in NPV for Portfolio B as compared with the RO/O case results.

It was observed that as tolerable risk was reduced, the robust designs obtained became sensitive to tolerable risk. Thus, robust optimal designs emerged that differed from those obtained for greater tolerable risk levels. As previously stated, this was expected; because, as the feasible set becomes more restricted, there may be a cost associated with a robust design in addition to a robust allocation due to how the design and crop allocation variables are coupled in the objective and capacity constraint functions. For Portfolio A, this was observed for the RO/RO case with $< 22.5\%$ tolerable risk (see Supplementary Information), quantified by the difference in NPVs between the RO/O and O/O cases. Similar behavior was observed for Portfolio B for tolerable risk below 23%. Interestingly, for the tolerable risk levels of 10% and 14%, the RO/RO and RO/O cases yielded the same NPV. Again, this is the result of a greater degree of coupling between the design and crop allocations from having mixed growing modes. This indicates that the incorporation of mushrooms dramatically reduces risk exposure at the cost of having mixed growing modes that are fixed at the design stage.

To assess the performance of the Portfolio A CEA system's robust crop allocations against naïve allocations, a Monte Carlo simulation with 5×10^5 realizations of market uncertainty $\mathbf{M}$ was performed, but the naïve strategy was preferred in this case as the worst-case risk of the naïve portfolio under expected market conditions was less than the worst-case risk of the robust solution. The resulting performance for the first two years (i.e., eight quarters) of the project horizon, which are repeated over the full 30-year project horizon, for this case can be viewed in the Supplementary Information.

Solution of (19) for the Portfolio B CEA system yielded disparate robust designs $\mathbf{d}^*$ over the range of tolerable risk levels tested: designs heavily favoring mushrooms for tolerable risk levels below 14% and far less so for tolerable risk levels above 21.75%. These results are likely due to nonconvexity, nonsmoothness, and possibly disconnectedness of the feasible set. Although cases between 14% and 21.75% are expected to be feasible, no solutions of (19) could be obtained within reasonable computation time (≤ 1 h). To assess the performance of the Portfolio B CEA system's robust crop allocations against naïve allocations, a Monte Carlo simulation with 5×10^5 realizations of market uncertainty $\mathbf{M}$ was performed for each design. The resulting performance for the first two years (i.e., eight quarters) of the project horizon, which are repeated over the

Table 2
Multi-scenario economic performance comparison for Portfolios A and B is tabulated for the robust optimal design with robust optimal allocations (RO/RO), robust optimal design with naïve allocations (RO/N), robust optimal design with optimal allocations (RO/O), and optimal design with optimal allocations (O/O). RO/RO results are reported as NPVs in million USD. All other results are reported as percentages of the RO/RO NPV.

Tolerable Risk	10%	14%	21.75%	22.5%	23%	25%
Portfolio A						
RO/RO [10^6 USD]	–	–	17.81	20.48	21.42	21.68
RO/N	–	–	−195%	−165%	−157%	−155%
RO/O	–	–	+12.6%	+5.7%	+1.0%	+0.0%
O/O	–	–	+21.5%	+5.7%	+1.0%	+0.0%
Portfolio B						
RO/RO [10^6 USD]	9.49	9.49	19.64	21.16	21.28	21.28
RO/N	−116%	−116%	−201%	−182%	−180%	−180%
RO/O	+0.0%	+0.0%	+1.3%	+0.7%	+0.0%	+0.0%
O/O	+124%	+124%	+8.5%	+0.8%	+0.0%	+0.0%

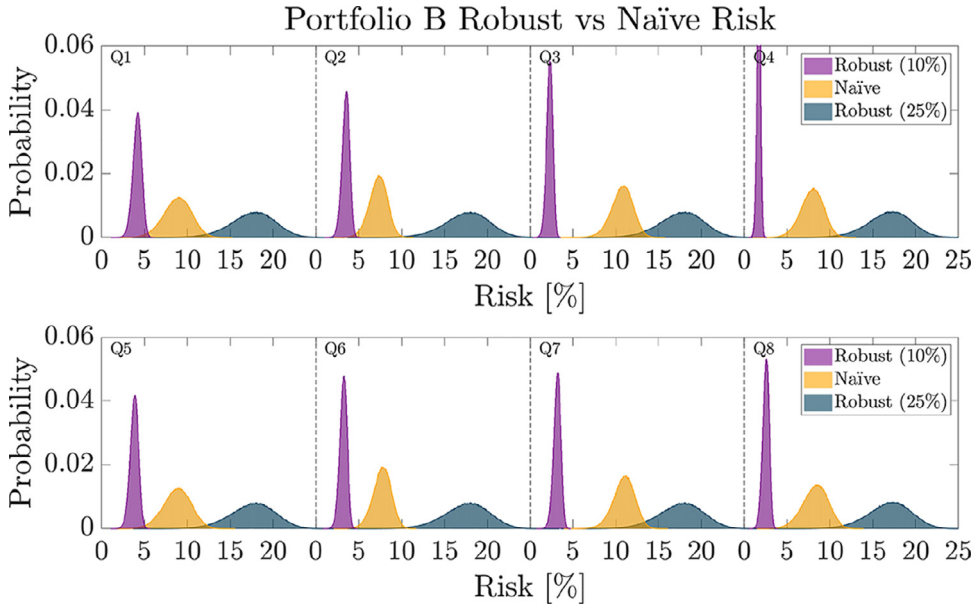

Fig. 9. Risk performance of Portfolio B is compared for naïve and robust (generated using 10% and 25% tolerable risk) portfolios for 5×10^5 realizations of expected market behavior over the March 1, 2018–March 1, 2020 planning horizon.

full 30-year project horizon, are shown in Fig. 9 for the relatively low-risk and high-risk designs for Portfolio B. Risk performance of the Portfolio B CEA system with 10% tolerable risk exposure shows similar results to the Portfolio A system with 25% tolerable risk exposure. For the lower-risk (10% tolerable risk) design case of Portfolio B, the expected risk distribution of robust crop allocations is shifted lower by an average of 5.6 percentage points and is narrowed as compared with the naïve portfolio. In all eight quarters the worst-case performance (highest risk) of the robust portfolios is approximately equal to or less than the best-case performance (lowest risk) of the naïve portfolios, which demonstrates a clear advantage of the robust portfolios from a risk perspective.

The higher-risk design case (25% tolerable risk), however, shows a different result. In this case the expected risk distribution of robust crop allocations is shifted higher than the naïve allocations by an average of 8.0 percentage points and is widened as compared with the naïve portfolio. This behavior arises as a consequence of robust portfolios that grow an overwhelming majority of tomatoes which are a higher-risk crop than mushrooms, for example, whose contribution to the naïve portfolio brings its risk below that of the portfolio that overwhelmingly favors tomatoes. In general, this type of result is possible when a robust optimal solution is obtained in any case where the tolerable risk level has been set higher than the worst-case risk exposure that can be expected with the naïve portfolio. For this reason, it is important to consider the expected risk of the naïve portfolio prior to tolerable risk level selection and robust optimization, which can be done easily using our presented methods.

5. Conclusion

In this work, a new methodology was developed for designing CEA systems robust to market uncertainty. To do this, an investor's approach (i.e., the trader's perspective for robust optimization of crop-specific commodities portfolios based on MPT), was first considered to validate diversification as an effective risk mitigation strategy for crop portfolios. Application of this so-called trader's method to two case studies revealed that significant portfolio risk reduction was achievable using this approach, thereby enabling its extension to a grower's perspective. The so-called Grower's Model was formulated as a nonconvex SIP and considers the simultaneous up-front design (scale and location) and long-term operation (growing decisions) of a CEA system. Application of the grower's method to two case studies revealed that this method effectively increased the robustness of CEA systems to market uncertainty, improved the long-term economics of CEA systems over naïve oper-

ating strategies, and validated the economic viability of single and dual-cultivation-mode CEA systems for production of distinct crop portfolios.

The flexibility of our approach enables robust optimization of CEA systems composed of any number of cultivation modes for production of any crop portfolio for which historical pricing data is known and capital and operating expenses can be estimated. As the first robust optimization approach to CEA systems, we believe this approach not only offers valuable economic insight to guide decision-making in CEA technology adoption, but also serves as a general framework for continued development of CEA decision-making models.

Declaration of Competing Interest

The authors declare that they have no known competing financial interests or personal relationships that could have appeared to influence the work reported in this paper.

CRediT authorship contribution statement

Shaylin A. Cetegen: Methodology, Software, Formal analysis, Investigation, Writing - original draft, Writing - review & editing, Data curation, Visualization. **Matthew D. Stuber:** Conceptualization, Methodology, Project administration, Software, Investigation, Validation, Resources, Supervision, Visualization, Writing - original draft, Writing - review & editing.

Acknowledgments

The authors would like to thank Matthew Wilhelm for his contributions to formulating the Grower's Problem economic objective function and for providing EAGO software support.

Funding: This research did not receive any specific grant from funding agencies in the public, commercial, or not-for-profit sectors.

Supplementary material

Supplementary material associated with this article can be found, in the online version, at 10.1016/j.compchemeng.2021.107285

References

Ahumada, O., Villalobos, J.R., 2009. Application of planning models in the agri-food supply chain: a review. Eur. J. Oper. Res. 196 (1), 1–20. doi:10.1016/j.ejor.2008.02.014.

Annevelink, E., 1992. Operational planning in horticulture: optimal space allocation in pot-plant nurseries using heuristic techniques. J. Agric. Eng. Res. 51, 167–177. doi:10.1016/0021-8634(92)80035-Q.

Bemporad, A., Filippi, C., 2006. An algorithm for approximate multiparametric convex programming. Comput. Optim. Appl. 35 (1), 87–108. doi:10.1007/s10589-006-6447-z.

Ben-Tal, A., Nemirovski, A., 1998. Robust convex optimization. Math. Oper. Res. 23 (4), 769–805. doi:10.1287/moor.23.4.769.

Benke, K., Tomkins, B., 2017. Future food-production systems: vertical farming and controlled-environment agriculture. Sustainability 13 (1), 13–26. doi:10.1080/15487733.2017.1394054.

Bezanson, J., Edelman, A., Karpinski, S., Shah, V.B., 2017. Julia: a fresh approach to numerical computing. SIAM Rev. 59 (1), 65–98. doi:10.1137/141000671.

Bhattacharjee, B., Green, W.H., Barton, P.I., 2005. Interval methods for semi-infinite programs. Comput. Optim. Appl. 30 (1), 63–93. doi:10.1007/s10589-005-4556-8.

Bhattacharjee, B., Lemonidis, P., Green Jr., W.H., Barton, P.I., 2005. Global solution of semi-infinite programs. Math. Program. 103 (2), 283–307. doi:10.1007/s10107-005-0583-6.

Biswas, A., Pal, B.B., 2005. Application of fuzzy goal programming technique to land use planning in agricultural system. Omega 33 (5), 391–398. doi:10.1016/j.omega.2004.07.003.

Blankenship, J.W., Falk, J.E., 1976. Infinitely constrained optimization problems. J. Optim. Theory Appl. 19 (2), 261–281. doi:10.1007/BF00934096.

Butturini, M., Marcelis, L.F.M., 2020. Vertical farming in Europe: present status and outlook. In: Plant Factory. Elsevier, pp. 77–91. doi:10.1016/B978-0-12-816691-8.00004-2.

Deschênes, O., Greenstone, M., 2007. The economic impacts of climate change: evidence from agricultural output and random fluctuations in weather. Am. Econ. Rev. 97 (1), 354–385. doi:10.1257/aer.97.1.354.

Despommier, D., 2009. The rise of vertical farms. Sci. Am. 301 (5), 80–87. doi:10.1038/scientificamerican1109-80.

Dua, V., Papalexandri, K.P., Pistikopoulos, E.N., 2004. Global optimization issues in multiparametric continuous and mixed-integer optimization problems. J. Glob. Optim. 30 (1), 59–89. doi:10.1023/b:jogo.0000049091.73047.7e.

Dunning, I., Huchette, J., Lubin, M., 2017. JuMP: a modeling language for mathematical optimization. SIAM Rev. 59 (2), 295–320. doi:10.1137/15M1020575.

Dury, J., Schaller, N., Garcia, F., Reynaud, A., Bergez, J.E., 2012. Models to support cropping plan and crop rotation decisions. A review. Agron. Sustain. Dev. 32 (2), 567–580. doi:10.1007/s13593-011-0037-x.

Falk, J.E., Hoffman, K., 1977. A nonconvex max-min problem. Nav. Res. Logist. Q. 24 (3), 441–450. doi:10.1002/nav.3800240307.

Fedoroff, N.V., 2015. Food in a future of 10 billion. Agric. Food Secur. 4 (1), 11. doi:10.1186/s40066-015-0031-7.

Field, C.B., Barros, V., Stocker, T.F., Dahe, Q., 2012. Managing the Risks of Extreme Events and Disasters to Advance Climate Change adaptation: Special Report of the Intergovernmental Panel on Climate Change (IPCC). Cambridge University Press.

Food and Agriculture Organization of the United Nations (FAO), 2018. The state of agricultural commodity markets 2018: Agricultural Trade, Climate Change and Food Security. Technical Report. FAO. URL http://www.fao.org/3/I9542EN/i9542en.pdf.

Glen, J.J., 1987. Mathematical models in farm planning: a survey. Oper. Res. 35 (5), 641–666. doi:10.1287/opre.35.5.641.

Gómez, C., Currey, C.J., Dickson, R.W., Kim, H.-J., Hernández, R., Sabeh, N.C., Raudales, R.E., Brumfield, R.G., Laury-Shaw, A., Wilke, A.K., Lopez, R.G., Burnett, S.E., 2019. Controlled environment food production for urban agriculture. HortScience 54 (9), 1448–1458. doi:10.21273/HORTSCI14073-19.

Grancharova, A., Johansen, T.A., 2006. Explicit approximate approach to feedback min-max model predictive control of constrained nonlinear systems. In: Proceedings of the 45th IEEE Conference on Decision and Control. IEEE doi:10.1109/cdc.2006.377772.

Grand View Research, 2019. Vertical farming market worth $9.96 billion by 2025. URL https://www.grandviewresearch.com/press-release/global-vertical-farming-market. Accessed: 2020- 05-21.

Gurobi Optimization, LLC, 2020. Gurobi optimizer reference manual. URL http://www.gurobi.com

Halemane, K.P., Grossmann, I.E., 1983. Optimal process design under uncertainty. AIChE J. 29 (3), 425–433. doi:10.1002/aic.690290312.

Hamer, P.J., 1994. A decision support system for the provision of planting plans for brussels sprouts. Comput. lectron. Agric. 11 (2-3), 97–115. doi:10.1016/0168-1699(94)90001-9.

Li, Z., Ierapetritou, M., 2008. Process scheduling under uncertainty: review and challenges. Comput. Chem. Eng. 32 (4-5), 715–727. doi:10.1016/j.compchemeng.2007.03.001.

Markowitz, H., 1952. Portfolio selection. J. Finance 7 (1), 77–91. doi:10.1111/j.1540-6261.1952.tb01525.x.

McCormick, G.P., 1976. Computability of global solutions to factorable nonconvex programs: part I–convex underestimating problems. Math. Program. 10 (1), 147–175. doi:10.1007/BF01580665.

Miles, P.G., Chang, S.-T., 2004. Mushrooms: Cultivation, Nutritional Value, Medicinal Effect, and Environmental Impact. CRC Press, Boca Raton, FL.

Mitsos, A., 2011. Global optimization of semi-infinite programs via restriction of the right-hand side. Optimization 60 (10-11), 1291–1308. doi:10.1080/02331934.2010.527970.

Nie, Y., Avraamidou, S., Xiao, X., Pistikopoulos, E.N., Li, J., Zeng, Y., Song, F., Yu, J., Zhu, M., 2019. A food-energy-water nexus approach for land use optimization. Sci. Total Environ. 659, 7–19. doi:10.1016/j.scitotenv.2018.12.242.

Oberdieck, R., Diangelakis, N.A., Nascu, I., Papathanasiou, M.M., Sun, M., Avraamidou, S., Pistikopoulos, E.N., 2016. On multi-parametric programming and its applications in process systems engineering. Chem. Eng. Res. Des. 116, 61–82. doi:10.1016/j.cherd.2016.09.034.

O'Donoghue, B., Chu, E., Parikh, N., Boyd, S., 2016. Conic optimization via operator splitting and homogeneous self-dual embedding. J. Optim. Theory Appl. 169 (3), 1042–1068. doi:10.1007/s10957-016-0892-3.

O'Donoghue, B., Chu, E., Parikh, N., Boyd, S., 2019. SCS: splitting conic solver, version 2.1.2. https://github.com/cvxgrp/scs.

Paut, R., Sabatier, R., Tchamitchian, M., 2019. Reducing risk through crop diversification: an application of portfolio theory to diversified horticultural systems. Agric. Syst. 168, 123–130. doi:10.1016/j.agsy.2018.11.002.

Pistikopoulos, E.N., 2009. Perspectives in multiparametric programming and explicit model predictive control. AIChE J. 55 (8), 1918–1925. doi:10.1002/aic.11965.

Rustem, B., Howe, M., 2002. Algorithms for Worst-Case Design and Applications to Risk Management. Princeton University Press, Princeton, NJ.

Stuber, M.D., Barton, P.I., 2015. Semi-infinite optimization with implicit functions. Ind. Eng. Chem. Res. 54, 307–317. doi:10.1021/ie5029123.

Stuber, M.D., Wechsung, A., Sundaramoorthy, A., Barton, P.I., 2014. Worst-case design of subsea production facilities using semi-infinite programming. AIChE J. 60 (7), 2513–2524. doi:10.1002/aic.14447.

Tridge, 2019. Market intelligence. URL https://www.tridge.com/prices. Accessed: 2020-05-21.
Wächter, A., Biegler, L.T., 2006. On the implementation of an interior-point filter line-search algorithm for large-scale nonlinear programming. Math. Program. 106 (1), 25–57. doi:10.1007/s10107-004-0559-y.
Wilhelm, M. E., Stuber, M. D., 2018. EAGO: easy advanced global optimization Julia package. URL https://github.com/PSORLab/EAGO.jl
Wilhelm, M.E., Stuber, M.D., 2020. EAGO.jl: easy advanced global optimization in Julia. Optim. Methods Softw. doi:10.1080/10556788.2020.1786566.
Žaković, S., Rustem, B., 2003. Semi-infinite programming and applications to minimax problems. Ann. Oper. Res. 124 (1-4), 81–110. doi:10.1023/b:anor.0000004764.76984.30.
Zeidler, C., Schubert, D., Vrakking, V., 2017. Vertical Farm 2.0: Designing an Economically Feasible Vertical Farm – A combined European Endeavor for Sustainable Urban Agriculture. Technical Report. Association for Vertical Farming. URL https://elib.dlr.de/116034/

Supplementary Information

Optimal Design of Controlled Environment Agricultural Systems Under Market Uncertainty

Shaylin A. Cetegen[a,1], Matthew D. Stuber[a,*]

[a]*Process Systems and Operations Research Laboratory, Dept. of Chemical and Biomolecular Engineering, University of Connecticut, 191 Auditorium Road, Unit 3222, Storrs, CT 06269, USA.*

---

1. Affine Relaxations of Non-affine and Non-bilinear Terms

In this section, we develop affine relaxations of the relevant terms of the grower's model objective function

$$f_{\text{NPV}}(\mathbf{d},\mathbf{X}) = C_{rev}(\mathbf{d},\mathbf{X}) - (1+P)C_{cap}(\mathbf{d}) - C_{op}(\mathbf{d},\mathbf{X}). \tag{1}$$

Only the functions

$$C_{cap,z}(\mathbf{d}) = C_{1,z}d_{z+2}^{0.9} + C_{2,z}d_{z+2} + G(\mathbf{d})d_{z+2} + C_{3,z},\ z = 1,\ldots,\mu \tag{2}$$

must be considered as all other functions consist only of bilinear or affine terms. Further, only the terms $u_{z+2} = d_{z+2}^{0.9}$, $z = 1,\ldots,\mu$, and the Gaussian function

$$G(\mathbf{d}) = S\exp\left(-x_{scale}(d_1)^2 + y_{scale}(d_2)^2\right) + S_{\min} \tag{3}$$

must be considered. Since the function $C_{cap}(\cdot)$ appears in $f_{\text{NPV}}(\cdot,\cdot)$ with a negative prefactor, and we are always maximizing $f_{\text{NPV}}(\cdot,\cdot)$, we must develop affine underestimators of $u_{z+2}(\cdot)$ and $G(\cdot)$ so that we can calculate valid upper bounds on the global optimal solution value f^* within the spatial branch-and-bound algorithm.

Definition 1 (Affine Underestimator/Relaxation)**.** *Let $Z \subset \mathbb{R}^n$ and let $f : Z \to \mathbb{R}$. An affine function $f^a : Z \to \mathbb{R}$ is called an* affine underestimator *or* affine relaxation *of f on Z if $f^A(\mathbf{z}) \leq f(\mathbf{z})$ for every $\mathbf{z} \in Z$.*

Definition 2. *For $q = 3,\ldots,\mu+2$, let $D_q = \{x \in \mathbb{R} : d_q^L \leq x \leq d_q^U\} = [d_q^L, d_q^U]$ and $u_q : D_q \to \mathbb{R} : d_q \mapsto d_q^{0.9}$. Then, for every $d_q \in D_q$, an affine relaxation of u_q on D_q is given by*

$$u_q^A(d_q) \equiv (d_q^L)^{0.9} + \frac{(d_q^U)^{0.9} - (d_q^L)^{0.9}}{d_q^U - d_q^L}(d_q - d_q^L). \tag{4}$$

Since u_q is strictly concave and scalar-valued, u_q^A is trivially the secant function defined between the points d_q^L and d_q^U.

To calculate affine relaxation of $G(\cdot)$ on D, we must define the concepts of convex relaxations and subgradients.

Definition 3 (Convex and Concave Relaxations (Mitsos et al., 2009))**.** *Given a convex set $Z \subset \mathbb{R}^n$ and a function $w : Z \to \mathbb{R}$, a convex function $w^{cv} : Z \to \mathbb{R}$ is a* convex relaxation of w on Z if $w^{cv}(\mathbf{z}) \leq w(\mathbf{z})$ for

*Corresponding author

Email addresses: cetegen@mit.edu (Shaylin A. Cetegen), stuber@alum.mit.edu (Matthew D. Stuber)

[1]Current address: Dept. of Chemical Engineering, Massachusetts Institute of Technology, 77 Massachusetts Ave., Cambridge, MA 02139, USA.

every $\mathbf{z} \in Z$. A concave function $w^{cc} : Z \to \mathbb{R}$ is a *concave relaxation* of w on Z if $w^{cc}(\mathbf{z}) \geq w(\mathbf{z})$ for every $\mathbf{z} \in Z$.

Definition 4 (Subgradients (Stuber et al., 2015)). *Let $Z \subset R^n$ be a nonempty convex set, $w^{cv} : Z \to \mathbb{R}$ be convex and $w^{cc} : Z \to \mathbb{R}$ be concave. A function $\mathbf{s}_w^{cv} : Z \to \mathbb{R}^n$ is a subgradient of w^{cv} on Z if for each $\bar{\mathbf{z}} \in Z, w^{cv}(\mathbf{z}) \geq w^{cv}(\bar{\mathbf{z}}) + \mathbf{s}_w^{cv}(\bar{\mathbf{z}})^{\mathrm{T}}(\mathbf{z} - \bar{\mathbf{z}}), \forall \mathbf{z} \in Z$. Similarly, a function $\mathbf{s}_w^{cc} : Z \to \mathbb{R}^n$ is a subgradient of w^{cc} on Z if for each $\bar{\mathbf{z}} \in Z, w^{cc}(\mathbf{z}) \leq w^{cc}(\bar{\mathbf{z}}) + \mathbf{s}_w^{cc}(\bar{\mathbf{z}})^{\mathrm{T}}(\mathbf{z} - \bar{\mathbf{z}}), \forall \mathbf{z} \in Z$.*

An affine relaxation of $G(\cdot)$ is then defined in the following.

Definition 5. *Let $D_1 = \{x \in \mathbb{R} : d_2^L \leq x \leq d_2^U\}$ and $D_2 = \{x \in \mathbb{R} : d_3^L \leq x \leq d_3^U\}$. Let $u_1^{cv} : D_1 \times D_2 \to \mathbb{R}$ be a convex relaxation of $u_1 = G$ on $D_1 \times D_2$. Let $\boldsymbol{\delta} = (d_1, d_2)$ and $\bar{\boldsymbol{\delta}} = (\bar{d}_1, \bar{d}_2)$ such that $\bar{d}_1 = (d_1^U + d_1^L)/2$ and $\bar{d}_2 = (d_2^U + d_2^L)/2$. Then, for every $\boldsymbol{\delta} \in D_1 \times D_2$, an affine relaxation of u_1 on $D_1 \times D_2$ is given by*

$$u_1^A(\boldsymbol{\delta}) \equiv u_1^{cv}(\bar{\boldsymbol{\delta}}) + \mathbf{s}_{u_1}^{cv}(\bar{\boldsymbol{\delta}})^{\mathrm{T}}(\boldsymbol{\delta} - \bar{\boldsymbol{\delta}}) \tag{5}$$

There are several ways to define convex relaxations (e.g., αBB (Adjiman and Floudas, 1996), auxiliary variable methods (Sahinidis, 1996), McCormick composition (McCormick, 1976), etc.). In this work, we utilize the McCormick-based library in EAGO (Wilhelm and Stuber, 2018, 2020) to construct and evaluate relaxations and subgradients.

Finally, a capital expense model only involving affine and bilinear terms is given by

$$\hat{C}_{cap,z}(\mathbf{d}) = C_{1,z} u_{z+2}^A(d_{z+2}) + C_{2,z} d_{z+2} + u_1^A(\boldsymbol{\delta}) d_{z+2} + C_{3,z}, \ z = 1, \ldots, \mu$$

where $\boldsymbol{\delta} = (d_1, d_2)$ as in Definition 5. Then, the relaxed objective, containing only linear and bilinear terms, is formulated as

$$\hat{f}_{\mathrm{NPV}}(\mathbf{d}, \mathbf{X}) = C_{rev}(\mathbf{d}, \mathbf{X}) - (1 + P) \sum_{z=1}^{\mu} \hat{C}_{cap,z}(\mathbf{d}) - C_{op}(\mathbf{d}, \mathbf{X}).$$

By construction, we have the following upper-bounding result:

$$\hat{f}_{\mathrm{NPV}}(\mathbf{d}, \mathbf{X}) \geq f_{\mathrm{NPV}}(\mathbf{d}, \mathbf{X}), \ \forall (\mathbf{d}, \mathbf{X}) \in D \times \Xi,$$

and so $\hat{f}_{\mathrm{NPV}}$ can be used to calculate valid upper bounds on the global optimal solution value within the spatial branch-and-bound algorithm.

2. Case-Study Numerical Values

Specific numerical values used to solve our model for the presented case studies are detailed in Table S1. $C_{1,1}$, $C_{2,1}$, $C_{3,1}$ and $C_{1,2}$, $C_{2,2}$, $C_{3,2}$ are all capital expense costs associated with cultivation modes 1 and 2, respectively.$C_{1,1}$ and $C_{1,2}$ are the volume-discountable capital expenses that scale with capacity. These values were calculated as the total sum of per-square-foot structural, illumination, horticultural equipment, and thermal management costs for the relevant cultivation mode that were derived based on proposed CEA systems presented by Zeidler et al. (2017) and Çelik and Peker (2009). $C_{2,1}$ and $C_{2,2}$ costs were not considered in this study but were presented in the formulation for generalization purposes. $C_{3,1}$ and $C_{3,2}$ costs represent the total sum of non-volume-discountable capital expenses that do not scale with capacity. In the case studies presented herein, the only qualified expense for this constant was the one-time upfront cost of purchasing a produce delivery truck for product distribution. This cost was associated with $C_{3,1}$ only since this cost does not need to be replicated as additional cultivation modes are added to the system.

Operating-cost-related parameters $I_{op,j,1}$ and $I_{op,j,2}$ represent the per-capacity quarterly operating expenses associated with cultivation modes 1 and 2, respectively. These values were calculated as the total sum of per-square-foot labor, energy, and horticultural materials costs for the relevant cultivation mode that were derived based on proposed CEA systems (Zeidler et al., 2017; Çelik and Peker, 2009). $F(\mathbf{d})$ are annual operating expenses that do not scale with capacity and are independent of the cultivation mode. The only

Parameter	Numerical Value	Units
μ	1 or 2 (Portfolio A or Portfolio B)	-
b	0.05/12	-
$C_{1,1}$	1192.3	USD
$C_{2,1}$	0.00	USD
$C_{3,1}$	70,000	USD
$C_{1,2}$	948.55	USD
$C_{2,2}$	0.00	USD
$C_{3,2}$	0.00	USD
$F(\mathbf{d})$	$1752.00(d_1 + d_2)$	USD
$I_{op,j,1}(\mathbf{x_j})$	$173.56+(39.96(x_{1j} + x_{2j}) + 6.91(x_{3j} + x_{4j}))$	USD
$I_{op,j,2}(\mathbf{x_j})$	160.36	USD
n_l	15	years
n_p	8	-
n_y	30	years
$p_{\min}$	(0.1, 0.1, 0.1, 0.1, 0.1)	-
$p_{\max}$	[10 10 10 10 10]	-
r_d	0.12	-
S	764	USD
$S_{\min}$	5.00	USD
x_{scale}	0.028	-
y_{scale}	0.031	-
$\mathbf{Y}$	$(25.05, 3.76, 100.16, 6.26, 62.6)^*$	pounds/sq.ft.
$\mathbf{w}$	$(2.5, 5.0, 4.0, 6.5, 10.0)^*$	USD/pound

Table S1: Numerical values used in robust optimization from the grower's and trader's perspectives. * indicates diagonal entries of the corresponding matrix $\in \mathbb{R}^{n_c \times n_c}$ are reported as a vector $\in \mathbb{R}^{n_c}$

such cost considered in this model was the distribution cost which depends on location design variables (d_1, d_2).

Crop allocation decision-making was performed over an n_p quarter planning horizon. The resulting allocations were repeated to span the n_y year project horizon over which the NPV of the full CEA system was calculated. It was assumed that capital financing was amortized monthly at an interest rate of b, discounted annually at a cash flow discount rate of r_d, and was paid off over the first n_l years of the project horizon. Additionally annual production of each crop was limited to between 0.1-10% of the annual market demand for the greater Boston area based on daytime population and land-cost parameters S, $S_{\min}$, x_{scale}, and y_{scale} were derived based on fitting the model to publicly-available land cost data for the greater Boston and surrounding area. Finally, CEA yield estimates for each crop on a pound-per-square-foot-of-land-footprint basis and expected market prices on a USD-per-pound basis were estimated based on previous studies and current market prices, respectively (Zeidler et al., 2017; Çelik and Peker, 2009).

3. Extended Results

Extended robust optimization results from the trader's and grower's models are reported in detail in Sections 3.1 and 3.2, respectively. The reported results contain multiple references to crops 1, 2, 3, 4, and 5 which correspond to lettuce, spinach, tomatoes, strawberries, and mushrooms, respectively.

3.1. Trader's Results

The following are the robust optimization results for 12 independent studies of Portfolios A and B simulated over planning horizons spanning from April 1, 2017 to March 1, 2020. The trader's model was run with a fixed tolerable risk level of 25% in all cases over 12 independent two-year planning horizons spanning from April 1, 2017 to March 1, 2020. The trader's model results include quarterly expected return, quarterly worst-case risk, and quarterly crop allocations.

3.1.1. Portfolio A Results

Planning horizon: April 1, 2017 - April 1, 2019 (See Table S2)

Planning horizon: May 1, 2017 - May 1, 2019 (See Table S3)

Planning horizon: June 1, 2017 - June 1, 2019 (See Table S4)

Planning horizon: July 1, 2017 - July 1, 2019 (See Table S5)

Planning horizon: August 1, 2017 - August 1, 2019 (See Table S6)

Planning horizon: September 1, 2017 - September 1, 2019 (See Table S7)

Planning horizon: October 1, 2017 - October 1, 2019 (See Table S8)

Planning horizon: November 1, 2017 - November 1, 2019 (See Table S9)

Planning horizon: December 1, 2018 - December 1, 2019 (See Table S10)

Planning horizon: January 1, 2018 - January 1, 2020 (See Table S11)

Planning horizon: February 1, 2018 - February 1, 2020 (See Table S12)

Planning horizon: March 1, 2018 - March 1, 2020 (See Table S13)

Quarter	Returns [%]	Risk [%]	Crop 1	Crop 2	Crop 3	Crop 4
Q1	3.4	9.6	0	0.90	0.10	0
Q2	2.9	5.5	0	0.98	0.02	0
Q3	3.4	6.1	0.08	0.88	0.04	0
Q4	6.7	23.9	0.44	0.04	0.52	0
Q5	2.0	9.9	0	0.84	0.14	0.02
Q6	2.0	6.7	0	0.96	0	0.04
Q7	2.2	6.1	0.08	0.88	0.04	0
Q8	6.0	25.9	0	0.43	0.55	0.03

Table S2: Trader's perspective robust optimization results for Portfolio A simulated over April 1, 2017 - April 1, 2019 planning horizon.

Quarter	Returns [%]	Risk [%]	Crop 1	Crop 2	Crop 3	Crop 4
Q1	3.2	7.9	0	0.94	0.06	0
Q2	3.9	5.4	0.26	0.72	0.02	0
Q3	5.5	11.8	0.35	0.36	0.29	0
Q4	11.4	23.6	0.37	0	0.28	0.35
Q5	2.0	8.4	0.01	0.85	0.12	0.02
Q6	3.0	5.5	0.31	0.69	0	0
Q7	2.0	7.0	0.02	0.98	0	0
Q8	10.8	26.4	0	0.3	0.41	0.29

Table S3: Trader's perspective robust optimization results for Portfolio A simulated over May 1, 2017 - May 1, 2019 planning horizon.

Quarter	Returns [%]	Risk [%]	Crop 1	Crop 2	Crop 3	Crop 4
Q1	4.0	8.7	0	0.91	0.05	0.04
Q2	2.9	4.0	0	0.96	0.04	0
Q3	2.0	6.7	0	0.96	0.04	0
Q4	7.9	21.2	0	0.21	0.6	0.19
Q5	2.0	8.8	0	0.94	0.03	0.03
Q6	2.0	4.0	0.10	0.90	0	0
Q7	3.5	10.4	0.10	0.90	0	0
Q8	9.3	21.3	0	0.2	0.6	0.2

Table S4: Trader's perspective robust optimization results for Portfolio A simulated over June 1, 2017 - June 1, 2019 planning horizon.

Quarter	Returns [%]	Risk [%]	Crop 1	Crop 2	Crop 3	Crop 4
Q1	2.9	5.5	0	0.98	0.02	0
Q2	3.4	6.1	0.08	0.88	0.04	0
Q3	6.7	23.9	0.44	0.04	0.52	0
Q4	2	9.9	0	0.84	0.14	0.02
Q5	2	6.7	0	0.96	0	0.04
Q6	2.2	6.1	0.08	0.88	0.04	0
Q7	6.0	25.9	0	0.43	0.55	0.02
Q8	2.0	10.0	0	0.99	0.01	0

Table S5: Trader's perspective robust optimization results for Portfolio A simulated over July 1, 2017 - July 1, 2019 planning horizon.

Quarter	Returns [%]	Risk [%]	Crop 1	Crop 2	Crop 3	Crop 4
Q1	3.9	5.4	0.26	0.72	0.02	0
Q2	3.0	6.9	0	1.0	0	0
Q3	11.4	23.6	0.37	0	0.28	0.35
Q4	2	8.3	0.01	0.85	0.12	0.02
Q5	3.0	5.5	0.31	0.69	0	0
Q6	2	7.0	0.02	0.98	0	0
Q7	10.8	26.4	0	0.3	0.41	0.29
Q8	2.3	7.9	0	0.94	0.06	0

Table S6: Trader's perspective robust optimization results for Portfolio A simulated over August 1, 2017 - August 1, 2019 planning horizon.

Quarter	Returns [%]	Risk [%]	Crop 1	Crop 2	Crop 3	Crop 4
Q1	2.9	4.0	0	0.96	0.04	0
Q2	2	6.7	0	0.96	0.04	0
Q3	7.9	21.2	0	0.21	0.6	0.19
Q4	2	8.8	0	0.94	0.03	0.03
Q5	2	4.0	0.10	0.90	0	0
Q6	3.5	10.4	0.09	0.8	0.11	0
Q7	9.5	21.1	0.04	0.19	0.57	0.2
Q8	2.5	8.8	0	0.96	0.02	0.02

Table S7: Trader's perspective robust optimization results for Portfolio A simulated over September 1, 2017 - September 1, 2019 planning horizon.

Quarter	Returns [%]	Risk [%]	Crop 1	Crop 2	Crop 3	Crop 4
Q1	3.4	6.1	0.08	0.88	0.04	0
Q2	6.7	23.5	0.44	0.03	0.52	0
Q3	2	9.9	0	0.84	0.14	0.02
Q4	2	6.7	0	0.96	0	0.04
Q5	2.2	6.1	0.08	0.88	0.04	0
Q6	6.0	25.6	0	0.43	0.55	0.02
Q7	2.3	6.7	0	1.0	0	0
Q8	2.3	6.7	0	1.0	0	0

Table S8: Trader's perspective robust optimization results for Portfolio A simulated over October 1, 2017 - October 1, 2019 planning horizon.

Quarter	Returns [%]	Risk [%]	Crop 1	Crop 2	Crop 3	Crop 4
Q1	5.5	11.8	0.35	0.36	0.29	0
Q2	11.4	23.6	0.37	0	0.28	0.35
Q3	2	8.4	0.01	0.85	0.12	0.02
Q4	3	5.5	0.31	0.69	0	0
Q5	2	7	0.02	0.98	0	0
Q6	10.8	26.4	0	0.3	0.41	0.29
Q7	2.3	7.9	0	0.94	0.06	0
Q8	2.6	6.0	0.04	0.96	0	0

Table S9: Trader's perspective robust optimization results for Portfolio A simulated over November 1, 2017 - November 1, 2019 planning horizon.

Quarter	Returns [%]	Risk [%]	Crop 1	Crop 2	Crop 3	Crop 4
Q1	2	6.7	0	0.96	0.04	0
Q2	7.9	21.2	0	0.21	0.6	0.19
Q3	2	8.8	0	0.94	0.03	0.03
Q4	2	4.0	0.1	0.9	0	0
Q5	3.5	10.4	0.09	0.8	0.11	0
Q6	9.3	21.3	0	0.2	0.6	0.2
Q7	2.5	8.8	0	0.97	0.02	0.01
Q8	2.5	4.0	0.02	0.98	0	0

Table S10: Trader's perspective robust optimization results for Portfolio A simulated over December 1, 2017 - December 1, 2019 planning horizon.

Quarter	Returns [%]	Risk [%]	Crop 1	Crop 2	Crop 3	Crop 4
Q1	6.7	23.9	0.44	0.03	0.52	0.01
Q2	2	9.9	0	0.84	0.14	0.02
Q3	2	6.7	0	0.96	0	0.04
Q4	2.2	6.1	0.08	0.88	0.04	0
Q5	6	25.9	0	0.43	0.55	0.02
Q6	2	10	0	0.99	0.01	0
Q7	2.3	6.7	0	1.0	0	0
Q8	2.7	6.2	0.03	0.93	0.04	0

Table S11: Trader's perspective robust optimization results for Portfolio A simulated over January 1, 2018 - January 1, 2020 planning horizon.

Quarter	Returns [%]	Risk [%]	Crop 1	Crop 2	Crop 3	Crop 4
Q1	11.4	23.6	0.37	0	0.28	0.35
Q2	2	8.3	0.01	0.85	0.12	0.02
Q3	3	5.5	0.31	0.69	0	0
Q4	2	7	0.02	0.98	0	0
Q5	10.8	26.4	0	0.3	0.41	0.29
Q6	2.3	7.9	0	0.94	0.06	0
Q7	2.6	6	0.04	0.96	0	0
Q8	2.5	6.9	0	1	0	0

Table S12: Trader's perspective robust optimization results for Portfolio A simulated over February 1, 2018 - February 1, 2020 planning horizon.

Quarter	Returns [%]	Risk [%]	Crop 1	Crop 2	Crop 3	Crop 4
Q1	7.9	21.2	0	0.21	0.6	0.19
Q2	2	8.8	0	0.94	0.03	0.03
Q3	2	4.0	0.1	0.9	0	0
Q4	3.5	10.4	0.09	0.8	0.11	0
Q5	9.5	21.1	0.04	0.19	0.57	0.2
Q6	2.5	8.8	0	0.96	0.02	0.02
Q7	2.5	4	0.02	0.98	0	0
Q8	3.2	10.4	0.09	0.8	0.11	0

Table S13: Trader's perspective robust optimization results for Portfolio A simulated over March 1, 2018 - March 1, 2020 planning horizon.

3.1.2. Portfolio B Results

Planning horizon: April 1, 2017 - April 1, 2019 (See Table S14)

Planning horizon: May 1, 2017 - May 1, 2019 (See Table S15)

Planning horizon: June 1, 2017 - June 1, 2019 (See Table S16)

Planning horizon: July 1, 2017 - July 1, 2019 (See Table S17)

Planning horizon: August 1, 2017 - August 1, 2019 (See Table S18)

Planning horizon: September 1, 2017 - September 1, 2019 (See Table S19)

Planning horizon: October 1, 2017 - October 1, 2019 (See Table S20)

Planning horizon: November 1, 2017 - November 1, 2019 (See Table S21)

Planning horizon: December 1, 2018 - December 1, 2019 (See Table S22

Planning horizon: January 1, 2018 - January 1, 2020 See Table S23)

Planning horizon: February 1, 2018 - February 1, 2020 (See Table S24)

Planning horizon: March 1, 2018 - March 1, 2020 (See Table S25)

Quarter	Returns [%]	Risk [%]	Crop 1	Crop 2	Crop 3	Crop 4	Crop 5
Q1	2.0	3.7	0	0.11	0.02	0.02	0.85
Q2	2.0	0.9	0	0	0	0.02	0.98
Q3	2.0	1.8	0.09	0.03	0	0	0.88
Q4	2.0	3.2	0	0.01	0.01	0.03	0.95
Q5	2.0	3.9	0.02	0.02	0	0.03	0.93
Q6	2.0	1.4	0	0	0	0.05	0.95
Q7	2.0	2.3	0.13	0	0	0.01	0.86
Q8	2.0	3.5	0.01	0	0.03	0.04	0.92

Table S14: Trader's perspective robust optimization results for Portfolio B simulated over April 1, 2017 - April 1, 2019 planning horizon.

Quarter	Returns [%]	Risk [%]	Crop 1	Crop 2	Crop 3	Crop 4	Crop 5
Q1	2.0	3.7	0.01	0.24	0.02	0	0.73
Q2	2.0	2.2	0.10	0	0	0	0.90
Q3	2.0	3.0	0.06	0.16	0	0	0.78
Q4	2.0	3.1	0	0	0	0.04	0.96
Q5	2.0	4.4	0.01	0.10	0.04	0.03	0.82
Q6	2.0	2.4	0.15	0	0	0	0.85
Q7	2.0	3.5	0.13	0	0.02	0	0.85
Q8	2.0	3.3	0	0	0	0.05	0.95

Table S15: Trader's perspective robust optimization results for Portfolio B simulated over May 1, 2017 - May 1, 2019 planning horizon.

Quarter	Returns [%]	Risk [%]	Crop 1	Crop 2	Crop 3	Crop 4	Crop 5
Q1	2.0	1.0	0	0	0	0.02	0.98
Q2	2.0	1.8	0.08	0.11	0	0	0.81
Q3	2.0	3.2	0.09	0	0.02	0	0.89
Q4	2.0	4.1	0	0	0	0.04	0.96
Q5	2.0	1.3	0	0	0	0.04	0.96
Q6	2.0	2.1	0.15	0	0	0	0.85
Q7	2.0	3.5	0.12	0	0.03	0	0.85
Q8	2.0	4.1	0	0	0	0.05	0.95

Table S16: Trader's perspective robust optimization results for Portfolio B simulated over June 1, 2017 - June 1, 2019 planning horizon.

Quarter	Returns [%]	Risk [%]	Crop 1	Crop 2	Crop 3	Crop 4	Crop 5
Q1	2.0	0.9	0	0	0	0.02	0.98
Q2	2.0	1.8	0.09	0.03	0	0	0.88
Q3	2.0	3.2	0	0.01	0.01	0.03	0.95
Q4	2.0	3.9	0.02	0.02	0	0.03	0.93
Q5	2.0	1.4	0	0	0	0.04	0.96
Q6	2.0	2.3	0.13	0	0	0.01	0.86
Q7	2.0	3.5	0.01	0	0.03	0.04	0.92
Q8	2.0	4.1	0.03	0.02	0	0.04	0.91

Table S17: Trader's perspective robust optimization results for Portfolio B simulated over July 1, 2017 - July 1, 2019 planning horizon.

Quarter	Returns [%]	Risk [%]	Crop 1	Crop 2	Crop 3	Crop 4	Crop 5
Q1	2.0	2.2	0.10	0	0	0	0.90
Q2	2.0	3.0	0.06	0.16	0	0	0.78
Q3	2.0	3.1	0	0	0	0.04	0.96
Q4	2.0	4.4	0.15	0	0	0	0.85
Q5	2.0	2.4	0.15	0	0	0	0.85
Q6	2.0	3.5	0.13	0	0.02	0	0.85
Q7	2.0	3.3	0	0	0	0.05	0.95
Q8	2.0	4.2	0	0.18	0.06	0.03	0.73

Table S18: Trader's perspective robust optimization results for Portfolio B simulated over August 1, 2017 - August 1, 2019 planning horizon.

Quarter	Returns [%]	Risk [%]	Crop 1	Crop 2	Crop 3	Crop 4	Crop 5
Q1	2.0	1.8	0.08	0.11	0	0	0.81
Q2	2.0	3.2	0.09	0	0.02	0	0.89
Q3	2.0	4.1	0	0	0	0.04	0.96
Q4	2.0	1.3	0	0	0	0.04	0.96
Q5	2.0	2.1	0.15	0	0	0	0.85
Q6	2.0	3.5	0.12	0	0.03	0	0.85
Q7	2.0	4.1	0	0	0	0.05	0.95
Q8	2.0	1.5	0	0	0	0.06	0.94

Table S19: Trader's perspective robust optimization results for Portfolio B simulated over September 1, 2017 - September 1, 2019 planning horizon.

Quarter	Returns [%]	Risk [%]	Crop 1	Crop 2	Crop 3	Crop 4	Crop 5
Q1	2.0	1.8	0.09	0.03	0	0	0.88
Q2	2.0	3.2	0	0.01	0.01	0.03	0.95
Q3	2.0	3.9	0.02	0.02	0	0.03	0.93
Q4	2.0	1.4	0	0	0	0.05	0.95
Q5	2.0	2.3	0.13	0	0	0.01	0.86
Q6	2.0	3.5	0.01	0	0.03	0.04	0.92
Q7	2.0	4.1	0.03	0.02	0	0.04	0.91
Q8	2.0	1.6	0	0	0	0.06	0.94

Table S20: Trader's perspective robust optimization results for Portfolio B simulated over October 1, 2017 - October 1, 2019 planning horizon.

Quarter	Returns [%]	Risk [%]	Crop 1	Crop 2	Crop 3	Crop 4	Crop 5
Q1	2.0	3.0	0.06	0.16	0	0	0.78
Q2	2.0	3.1	0	0	0	0.04	0.96
Q3	2.0	4.4	0.01	0.10	0.04	0.03	0.82
Q4	2.0	2.4	0.15	0	0	0	0.85
Q5	2.0	3.5	0.13	0	0.02	0	0.85
Q6	2.0	3.3	0	0	0	0.05	0.95
Q7	2.0	4.2	0	0.18	0.06	0.03	0.73
Q8	2.0	3.0	0.01	0	0.01	0.05	0.93

Table S21: Trader's perspective robust optimization results for Portfolio B simulated over November 1, 2017 - November 1, 2019 planning horizon.

Quarter	Returns [%]	Risk [%]	Crop 1	Crop 2	Crop 3	Crop 4	Crop 5
Q1	2.0	3.2	0.09	0	0.02	0	0.89
Q2	2.0	4.1	0	0	0	0.04	0.96
Q3	2.0	1.3	0	0	0	0.04	0.96
Q4	2.0	2.1	0.15	0	0	0	0.85
Q5	2.0	3.5	0.12	0	0.03	0	0.85
Q6	2.0	4.1	0	0	0	0.05	0.95
Q7	2.0	1.5	0	0	0	0.06	0.94
Q8	2.0	2.5	0.09	0.31	0	0	0.76

Table S22: Trader's perspective robust optimization results for Portfolio B simulated over December 1, 2017 - December 1, 2019 planning horizon.

Quarter	Returns [%]	Risk [%]	Crop 1	Crop 2	Crop 3	Crop 4	Crop 5
Q1	2.0	3.2	0	0.01	0.01	0.03	0.95
Q2	2.0	3.9	0.02	0.02	0	0.03	0.93
Q3	2.0	1.4	0	0	0	0.05	0.95
Q4	2.0	2.3	0.13	0	0	0.01	0.86
Q5	2.0	3.5	0.01	0	0.03	0.04	0.92
Q6	2.0	4.1	0.03	0.02	0	0.04	0.91
Q7	2.0	1.6	0	0	0	0.06	0.94
Q8	2.0	2.8	0.08	0.11	0.01	0.02	0.78

Table S23: Trader's perspective robust optimization results for Portfolio B simulated over January 1, 2018 - January 1, 2020 planning horizon.

Quarter	Returns [%]	Risk [%]	Crop 1	Crop 2	Crop 3	Crop 4	Crop 5
Q1	2.0	3.1	0	0	0	0.04	0.96
Q2	2.0	4.4	0.01	0.10	0.04	0.03	0.82
Q3	2.0	2.4	0.15	0	0	0	0.85
Q4	2.0	3.5	0.13	0	0.02	0	0.85
Q5	2.0	3.3	0	0	0	0.05	0.95
Q6	2.0	4.2	0.01	0.18	0.06	0.03	0.72
Q7	2.0	3.0	0.01	0	0.01	0.05	0.93
Q8	2.0	3.8	0.16	0.06	0	0	0.78

Table S24: Trader's perspective robust optimization results for Portfolio B simulated over February 1, 2018 - February 1, 2020 planning horizon.

Quarter	Returns [%]	Risk [%]	Crop 1	Crop 2	Crop 3	Crop 4	Crop 5
Q1	2.0	4.1	0	0	0	0.04	0.96
Q2	2.0	1.3	0	0	0	0.04	0.96
Q3	2.0	2.1	0.15	0	0	0	0.85
Q4	2.0	3.5	0.12	0	0.03	0	0.85
Q5	2.0	4.1	0	0	0	0.06	0.94
Q6	2.0	1.5	0	0	0	0.06	0.94
Q7	2.0	2.5	0.09	0.31	0	0	0.6
Q8	2.0	3.5	0.07	0.02	0.02	0.03	0.86

Table S25: Trader's perspective robust optimization results for Portfolio B simulated over March 1, 2018 - March 1, 2020 planning horizon.

3.2. Grower's Results

The following are the robust optimization results for three independent studies of Portfolio A and six independent studies of Portfolio B simulated for various tolerable risk levels over the same planning horizon spanning from March 1, 2018 to March 1, 2020. The grower's model was run for various tolerable risk levels between 22.5% and 25% for Portfolio A and between 10% and 25% for Portfolio B. The grower's model results include the optimal capacity, location, crop allocations, and NPV of the CEA system in addition to the capital expenses, non-discounted average quarterly operating expenses and revenue.

3.2.1. Portfolio A Results

Tolerable Quarterly Risk*	25%
Optimal Capacity	26,672 sq.ft.
Optimal Locations	0 miles west/east
	15.8 miles south/north
Optimal Crop Allocations	See Table S30
Optimal NPV	$21.68 million
Capital Expenses	$11.5 million
Average Quarterly Operating Expenses	$5.0 million
Average Quarterly Revenue	$9.94 million

Table S26: Grower's perspective robust optimization results for Portfolio A simulated over March 1, 2018 - March 1, 2020 planning horizon for 25% tolerable risk.
* See corresponding risk profiles in Figure S1

Tolerable Quarterly Risk	23%
Optimal Capacity	26,672 sq.ft.
Optimal Locations	0 miles west/east
	15.8 miles south/north
Optimal Crop Allocations	See Table S31
Optimal NPV	$21.42 million
Capital Expenses	$11.5 million
Average Quarterly Operating Expenses	$5.0 million
Average Quarterly Revenue	$9.91 million

Table S27: Grower's perspective robust optimization results for Portfolio A simulated over March 1, 2018 - March 1, 2020 planning horizon for 23% tolerable risk.

Tolerable Quarterly Risk	22.5%
Optimal Capacity	26,672 sq.ft.
Optimal Locations	0 miles west/east
	15.8 miles south/north
Optimal Crop Allocations	See Table S32
Optimal NPV	$20.48 million
Capital Expenses	$11.5 million
Average Quarterly Operating Expenses	$5.0 million
Average Quarterly Revenue	$9.79 million

Table S28: Grower's perspective robust optimization results for Portfolio A simulated over March 1, 2018 - March 1, 2020 planning horizon for 22.5% tolerable risk.

Tolerable Quarterly Risk	21.75%
Optimal Capacity	27,554 sq.ft.
Optimal Locations	0 miles west/east
	15.8 miles south/north
Optimal Crop Allocations	See Table S33
Optimal NPV	$17.82 million
Capital Expenses	$11.9 million
Average Quarterly Operating Expenses	$5.0 million
Average Quarterly Revenue	$9.72 million

Table S29: Grower's perspective robust optimization results for Portfolio A simulated over March 1, 2018 - March 1, 2020 planning horizon for 21.75% tolerable risk.

Quarter	Crop 1	Crop 2	Crop 3	Crop 4
Q1	0.0199	0.0287	0.932	0.0193
Q2	0.0191	0.0245	0.937	0.0193
Q3	0.0190	0.0242	0.940	0.0172
Q4	0.0304	0.0350	0.893	0.0419
Q5	0.0149	0.0190	0.945	0.0211
Q6	0.0219	0.0234	0.913	0.0413
Q7	0.0206	0.0219	0.938	0.0197
Q8	0.0310	0.0482	0.905	0.0157

Table S30: Robust optimal quarterly crop allocations for Portfolio A under 25% tolerable quarterly risk exposure simulated over March 1, 2018 - March 1, 2020 planning horizon.

Quarter	Crop 1	Crop 2	Crop 3	Crop 4
Q1	0.0114	0.0517	0.912	0.0252
Q2	8.04e-3	6.53e-3	0.972	0.0132
Q3	7.99e-3	6.54e-3	0.973	0.0121
Q4	0.0609	0.0477	0.844	0.0473
Q5	4.02e-6	0.0443	0.907	0.0489
Q6	6.27e-6	0.0443	0.907	0.0489
Q7	2.41e-6	2.12e-6	1.0	9.53e-6
Q8	0.0941	0.0422	0.864	5.66e-6

Table S31: Robust optimal quarterly crop allocations for Portfolio A under 23% tolerable quarterly risk exposure simulated over March 1, 2018 - March 1, 2020 planning horizon.

Quarter	Crop 1	Crop 2	Crop 3	Crop 4
Q1	8.15e-5	0.0847	0.892	0.0236
Q2	5.85e-5	4.51e-5	1.0	1.50e-4
Q3	5.85e-5	4.51e-5	1.0	1.49e-4
Q4	0.0882	0.0277	0.810	0.0738
Q5	1.46e-6	0.0793	0.872	0.0488
Q6	7.49e-6	0.0792	0.872	0.0489
Q7	1.02e-6	8.88e-7	1.0	3.26e-6
Q8	0.0938	0.0632	0.843	1.32e-5

Table S32: Robust optimal quarterly crop allocations for Portfolio A under 22.5% tolerable quarterly risk exposure simulated over March 1, 2018 - March 1, 2020 planning horizon.

Quarter	Crop 1	Crop 2	Crop 3	Crop 4
Q1	1.79e-5	0.133	0.795	0.0717
Q2	9.58e-6	7.31e-6	1.0	2.11e-5
Q3	9.58e-6	7.31e-6	1.0	2.1e-5
Q4	0.188	0.00194	0.788	0.0229
Q5	3.8e-6	0.161	0.791	0.0473
Q6	3.8e-6	0.161	0.791	0.0473
Q7	5.44e-6	4.7e-6	1.0	6.34e-6
Q8	0.0943	0.0941	0.812	7.2e-6

Table S33: Robust optimal quarterly crop allocations for Portfolio A under 21.75% tolerable quarterly risk exposure simulated over March 1, 2018 - March 1, 2020 planning horizon.

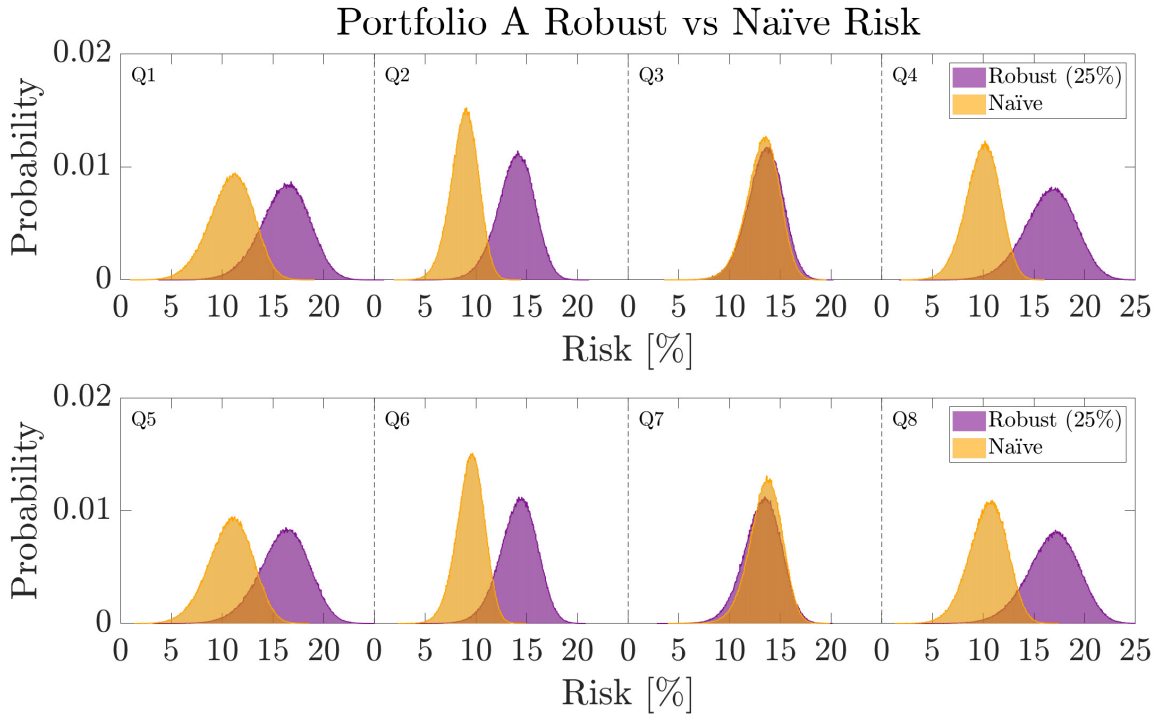

Figure S1: Risk performance of Portfolio A is compared for naïve and robust (generated using 25% tolerable risk) portfolios for $5{\cdot}10^5$ realizations of expected market behavior over the March 1, 2018 - March 1, 2020 planning horizon.

3.2.2. Portfolio B Results

Tolerable Quarterly Risk	25%
Optimal Capacity	26,747 sq.ft.
Optimal Locations	0 miles west/east
	15.8 miles south/north
Optimal Crop Allocations	See Table S40
Optimal NPV	$21.28 million
Capital Expenses	$11.7 million
Average Quarterly Operating Expenses	$5.0 million
Average Quarterly Revenue	$9.94 million

Table S34: Grower's perspective robust optimization results for Portfolio B simulated over March 1, 2018 - March 1, 2020 planning horizon for 25% tolerable risk.

Tolerable Quarterly Risk	23%
Optimal Capacity	26,747 sq.ft.
Optimal Locations	0 miles west/east
	15.8 miles south/north
Optimal Crop Allocations	See Table S41
Optimal NPV	$21.28 million
Capital Expenses	$11.7 million
Average Quarterly Operating Expenses	$5.0 million
Average Quarterly Revenue	$9.94 million

Table S35: Grower's perspective robust optimization results for Portfolio B simulated over March 1, 2018 - March 1, 2020 planning horizon for 23% tolerable risk.

Tolerable Quarterly Risk	22.5%
Optimal Capacity	26,747 sq.ft.
Optimal Locations	0 miles west/east
	15.8 miles south/north
Optimal Crop Allocations	See Table S42
Optimal NPV	$21.16 million
Capital Expenses	$11.7 million
Average Quarterly Operating Expenses	$4.9 million
Average Quarterly Revenue	$9.92 million

Table S36: Grower's perspective robust optimization results for Portfolio B simulated over March 1, 2018 - March 1, 2020 planning horizon for 22.5% tolerable risk.

Tolerable Quarterly Risk	21.75%
Optimal Capacity	27,556 sq.f.
Optimal Locations	0 miles west/east
	15.9 miles south/north
Optimal Crop Allocations	See Table S43
Optimal NPV	$19.64 million
Capital Expenses	$12.1 million
Average Quarterly Operating Expenses	$5.07 million
Average Quarterly Revenue	$10.0 million

Table S37: Grower's perspective robust optimization results for Portfolio B simulated over March 1, 2018 - March 1, 2020 planning horizon for 21.75% tolerable risk.

Tolerable Quarterly Risk	14%
Optimal Capacity	9,810 sq.ft.
Optimal Locations	0 miles west/east
	14.7 miles south/north
Optimal Crop Allocations	See Table S44
Optimal NPV	$9.49 million
Capital Expenses	$4.3 million
Average Quarterly Operating Expenses	$1.64 million
Average Quarterly Revenue	$3.70 million

Table S38: Grower's perspective robust optimization results for Portfolio B simulated over March 1, 2018 - March 1, 2020 planning horizon for 14% tolerable risk.

Tolerable Quarterly Risk	10%
Optimal Capacity	9,810 sq.ft.
Optimal Locations	0 miles west/east 14.7 miles south/north
Optimal Crop Allocations	See Table S45
Optimal NPV	$9.49 million
Capital Expenses	$4.3 million
Average Quarterly Operating Expenses	$1.64 million
Average Quarterly Revenue	$3.70 million

Table S39: Grower's perspective robust optimization results for Portfolio B simulated over March 1, 2018 - March 1, 2020 planning horizon for 10% tolerable risk.

Quarter	Crop 1	Crop 2	Crop 3	Crop 4	Crop 5
Q1	0.0318	0.0287	0.901	0.0353	0.00283
Q2	0.0198	0.0251	0.918	0.0342	0.00283
Q3	0.0245	0.026	0.921	0.0258	0.00283
Q4	0.012	0.0323	0.951	0.00209	0.00283
Q5	0.0112	0.00321	0.948	0.0345	0.00283
Q6	0.0202	0.0264	0.918	0.0323	0.00283
Q7	0.0283	0.0299	0.926	0.0128	0.00283
Q8	0.0285	0.0527	0.898	0.0179	0.00283

Table S40: Robust-optimal quarterly crop allocations for Portfolio B under 25% tolerable quarterly risk exposure simulated over March 1, 2018 - March 1, 2020 planning horizon.

Quarter	Crop 1	Crop 2	Crop 3	Crop 4	Crop 5
Q1	0.0126	0.0461	0.912	0.0270	0.00283
Q2	0.00938	0.00731	0.966	0.0147	0.00283
Q3	0.00924	0.0073	0.967	0.0134	0.00283
Q4	0.0569	0.0514	0.846	0.0424	0.00283
Q5	0.00697	0.0383	0.900	0.052	0.00283
Q6	0.0049	0.00447	0.971	0.0167	0.00283
Q7	0.00495	0.00446	0.973	0.015	0.00283
Q8	0.0713	0.0649	0.847	0.0138	0.00283

Table S41: Robust-optimal quarterly crop allocations for Portfolio B under 23% tolerable quarterly risk exposure simulated over March 1, 2018 - March 1, 2020 planning horizon.

Quarter	Crop 1	Crop 2	Crop 3	Crop 4	Crop 5
Q1	0.00155	0.0768	0.887	0.0318	0.00283
Q2	0.00103	8.04e-4	0.993	0.00222	0.00283
Q3	0.00103	8.03e-4	0.993	0.00218	0.00283
Q4	0.0845	0.0338	0.818	0.0613	0.00283
Q5	5.26e-6	0.0587	0.841	0.0975	0.00283
Q6	4.68e-7	4.18e-7	0.997	1.58e-6	0.00283
Q7	4.68e-7	4.18e-7	0.997	1.58e-6	0.00283
Q8	0.0936	0.0604	0.843	7.16e-6	0.00283

Table S42: Robust-optimal quarterly crop allocations for Portfolio B under 22.5% tolerable quarterly risk exposure simulated over March 1, 2018 - March 1, 2020 planning horizon.

Quarter	Crop 1	Crop 2	Crop 3	Crop 4	Crop 5
Q1	6.46e-6	0.127	0.801	0.0688	0.00275
Q2	1.41e-8	8.94e-9	0.997	3.34e-8	0.00275
Q3	1.41e-8	8.94e-9	0.997	3.34e-8	0.00275
Q4	0.185	3.57e-6	0.787	0.0259	0.00275
Q5	1.25e-6	0.126	0.777	0.0946	0.00275
Q6	1.95e-9	6.67e-10	0.997	1.61e-8	0.00275
Q7	1.95e-9	6.67e-10	0.997	1.61e-8	0.00275
Q8	0.0981	0.0878	0.811	3.05e-6	0.00275

Table S43: Robust-optimal quarterly crop allocations for Portfolio B under 21.75% tolerable quarterly risk exposure simulated over March 1, 2018 - March 1, 2020 planning horizon.

Quarter	Crop 1	Crop 2	Crop 3	Crop 4	Crop 5
Q1	0.0558	0.0607	0.0273	0.0843	0.772
Q2	0.0583	0.0774	0.0240	0.0683	0.772
Q3	0.0645	0.0864	0.0247	0.0525	0.772
Q4	0.0616	0.0812	0.0247	0.0606	0.772
Q5	0.0657	0.0811	0.0260	0.0554	0.772
Q6	0.0541	0.0745	0.0247	0.0748	0.772
Q7	0.0619	0.0788	0.0253	0.0621	0.772
Q8	0.0585	0.0715	0.0247	0.0734	0.772

Table S44: Robust-optimal quarterly crop allocations for Portfolio B under 14% tolerable quarterly risk exposure simulated over March 1, 2018 - March 1, 2020 planning horizon.

Quarter	Crop 1	Crop 2	Crop 3	Crop 4	Crop 5
Q1	0.0569	0.0652	0.0259	0.0801	0.772
Q2	0.0556	0.0775	0.0248	0.0703	0.772
Q3	0.0661	0.0817	0.0246	0.0557	0.772
Q4	0.0617	0.0815	0.0253	0.0597	0.772
Q5	0.0563	0.0608	0.0262	0.0849	0.772
Q6	0.0563	0.0785	0.0247	0.0687	0.772
Q7	0.0659	0.0829	0.0249	0.0544	0.772
Q8	0.0618	0.0835	0.0249	0.0578	0.772

Table S45: Robust-optimal quarterly crop allocations for Portfolio B under 10% tolerable quarterly risk exposure simulated over March 1, 2018 - March 1, 2020 planning horizon.

References

Claire S. Adjiman and Christodoulos A. Floudas. Rigorous convex underestimators for general twice-differentiable problems. *Journal of Global Optimization*, 9(1):23–40, jul 1996. doi:10.1007/BF00121749.

Yusuf Çelik and Kenan Peker. Benefit/cost analysis of mushroom production for diversification of income in developing countries. *Bulgarian Journal of Agricultural Science*, 15(3):228–237, 2009.

Garth P. McCormick. Computability of global solutions to factorable nonconvex programs: Part I-convex underestimating problems. *Math. Program*, 10:147–175, 1976. doi:10.1007/BF01580665.

Alexander Mitsos, Benoit Chachuat, and Paul I. Barton. McCormick-based relaxations of algorithms. *SIAM Journal of Optimization*, 20(2):573–601, December 2009. doi:10.1137/080717341.

Nikolaos V. Sahinidis. BARON: A general purpose global optimization software package. *Journal of Global Optimization*, 8(2):201–205, 1996. ISSN 1573-2916. doi:10.1007/BF00138693.

M. D. Stuber, J. K. Scott, and P. I. Barton. Convex and concave relaxations of implicit functions. *Optimization Methods and Software*, 30(3):424–460, 2015. doi:10.1080/10556788.2014.924514.

Matthew E. Wilhelm and Matthew D. Stuber. EAGO: Easy advanced global optimization Julia package, 2018. URL `https://github.com/PSORLab/EAGO.jl`.

Matthew E. Wilhelm and Matthew D. Stuber. EAGO.jl: Easy advanced global optimization in Julia. *Optimization Methods & Software*, Accepted, 2020. doi:10.1080/10556788.2020.1786566.

Conrad Zeidler, Daniel Schubert, and Vincent Vrakking. Vertical farm 2.0: Designing an economically feasible vertical farm – a combined european endeavor for sustainable urban agriculture. Technical report, 2017.